รายงานการวิจัยฉบับสมบูรณ์

อันตรกิริยาระหว่างยาต้านมะเร็งซิสพลาตินและโปรตีนบีอาร์ซีเอวันริงโดเมน

Interaction between the anticancer drug cisplatin and BRCA1 RING domain

หัวหน้าโครงการวิจัย

รองศาสตราจารย์ ดร. อดิศร รัตนพันธ์

โครงการวิจัยนี้ได้รับทุนอุดหนุนการวิจัยจากเงินรายได้มหาวิทยาลัยสงขลานครินทร์ ประเภททั่วไป ประจำปีงบประมาณ 2553

ABSTRACT

Tumor suppressor protein BRCA1 participates in genomic integrity maintenance through DNA repair, cell cycle checkpoint, protein ubiquitination, and transcriptional regulation. The N-terminus of BRCA1 contains a RING domain which forms two Zn^{2+}-binding sites in an interleaved fashion. Preclinical and clinical studies have recently revealed that the inactivation of BRCA1 in cancer cells leads to chemosensitivity. Therefore, approaching the BRCA1 RING domain as a potentially molecular target for a platinum-based drug might be of interest in cancer therapy. The *in vitro* platination of the BRCA1 RING domain by the anticancer drug cisplatin was observed. Cisplatin formed the intramolecular and intermolecular BRCA1 adducts by which His117 was the primary platinum-binding site. The apo form, not holo form, of BRCA1 underwent more folded structural rearrangement upon cisplatin binding. Cisplatin-modified BRCA1 also exhibited an enhanced thermostability, resulting from the favourably intermolecular cross-links driven by the free energy. The data could raise the possibility of selectively targeting the BRCA1 N-terminal domain for cancer therapy with less toxicity or improved response to conventional regimens.

บทคัดย่อ

โปรตีนกดการเกิดมะเร็ง BRCA1 ทำหน้าที่เกี่ยวข้องในการรักษาเสถียรภาพของจีโนมโดยอาศัยกระบวนการซ่อมแซมดีเอ็นเอที่เสียหาย การควบคุมวงรอบชีวิตของเซลล์ กระบวน การ ubiquitination และการควบคุมการถอดรหัส บริเวณด้านปลายอะมิโนของ BRCA1 เป็นส่วนที่เรียกว่า RING domain ซึ่งมีการจัดเรียงตัวของกรดอะมิโนในบริเวณดังกล่าวเพื่อจับกับโลหะสังกะสี 2 ตัว การศึกษาทางพรีคลินิกและทางคลินิกแสดงให้เห็นว่าการยับยั้งการทำงานของ BRCA1 ในเซลล์มะเร็งทำให้เซลล์มะเร็งไวต่อยาเคมีบำบัด ดังนั้นเป็นที่น่าสนใจที่ BRCA1 RING domain น่าจะเป็นเป้าหมายระดับโมเลกุลของยาในกลุ่มพลาตินัมในการรักษามะเร็ง การศึกษาในหลอดทดลองระหว่าง BRCA1 RING กับยาต้านมะเร็งซิสพลาตินพบว่าซิสพลาตินเกิดพันธะกับโปรตีน BRCA1 ทั้งภายในและระหว่างโมเลกุล BRCA1 โดยที่อะตอมพลาตินัมของซิสพลาตินเกิดพันธะกับกรดอะมิโนฮิสติดีนที่ตำแหน่ง 117 ของ BRCA1 RING domain BRCA1ในสภาวะที่ไม่มีโลหะสังกะสีเท่านั้นที่มีโครงสร้างที่ม้วนตัวมากขึ้นเมื่อเกิดอันตรกิริยากับซิสพลาติน ซิสพลาตินยังทำให้ BRCA1 มีความคงตัวต่อความร้อนเพิ่มขึ้นเนื่องจากการเกิดพันธะระหว่างโมเลกุลของ BRCA1 กับซิสพลาติน ข้อมูลที่ได้เหล่านี้อาจเพิ่มความเป็นไปได้ที่ BRCA1 N-terminal domain เป็นเป้าหมายจำเพาะสำหรับการรักษามะเร็งเพื่อลดความเป็นพิษของยาให้น้อยลงหรือเพิ่มผลการตอบสนองของยากลุ่มเดิม

ACKNOWLEDGMENTS

This work was supported by Prince of Songkla University (PHA530188S). The author would like to thank Prof. Dr. Udo Heinemann at Max-Delbrück Center for Molecular Medicine (Berlin, Germany) for kind assistance and support, and the Pharmaceutical Laboratory Service Center, Faculty of Pharmaceutical Sciences, Prince of Songkla University for research facilities.

Adisorn Ratanaphan

CONTENTS

INTRODUCTION

Cisplatin or *cis*-diamminedichloroplatinum(II), a platinum-based anticancer drug (Fig. 1), is widely used for the treatment against human testicular, bladder, ovarian, and head and neck cancers [1]. Its anticancer activity potentially results from the modification of DNA through covalent cross-linkings or platinum-DNA adducts which interfere DNA replication, transcription and ultimately lead to cancer cell death [2-4]. The effectiveness of the anticancer drug cisplatin depends on the drug uptake and its actual amount that reacts with the cellular targets. The physiological chloride concentration (100 mM) in blood and extracellular fluids is high enough to suppress cisplatin hydrolysis. Cisplatin reaches the surface of cells as a dichloro form. Passive diffusion is believed to be the main mechanism that enables it to enter the cells. The drug uptake in the breast cancer MCF-7 cells was 0.197 ng platinum per mg protein with a high accumulation ratio of 5.04 between the intracellular and extracellular platinum concentrations after a 24 h continuous treatment with cisplatin (0.1 μM) [5]. The intracellular activation of cisplatin is required before it plays an important role in cytotoxicity, facilitating by the low cellular concentration of chloride ions about 2-3 mM. Chlorine groups of cisplatin are easily replaced by water molecules to allow the formation of aqauted species in a stepwise manner. The hydration rate constant of monoaqua form was faster than that of diaqua form (2.38×10^{-5} s^{-1} compared to 1.4×10^{-5} s^{-1}) [6]. The aqauted forms are more reactive to the cellular targets which contain nucleophilic groups such as DNA and RNA at N7 position of guanine and adenine bases and protein side-chains of cysteine, methionine and histidine at sulfur and nitrogen moieties (Fig. 2)[7].

The interaction of cisplatin with proteins is of particular significance and believed to play an important role in drug distribution and inactivation responsible for determining its toxicity [8-15]. Intriguingly, its reaction also implicates in some crucial aspects of protein structures and functions (Table 1).

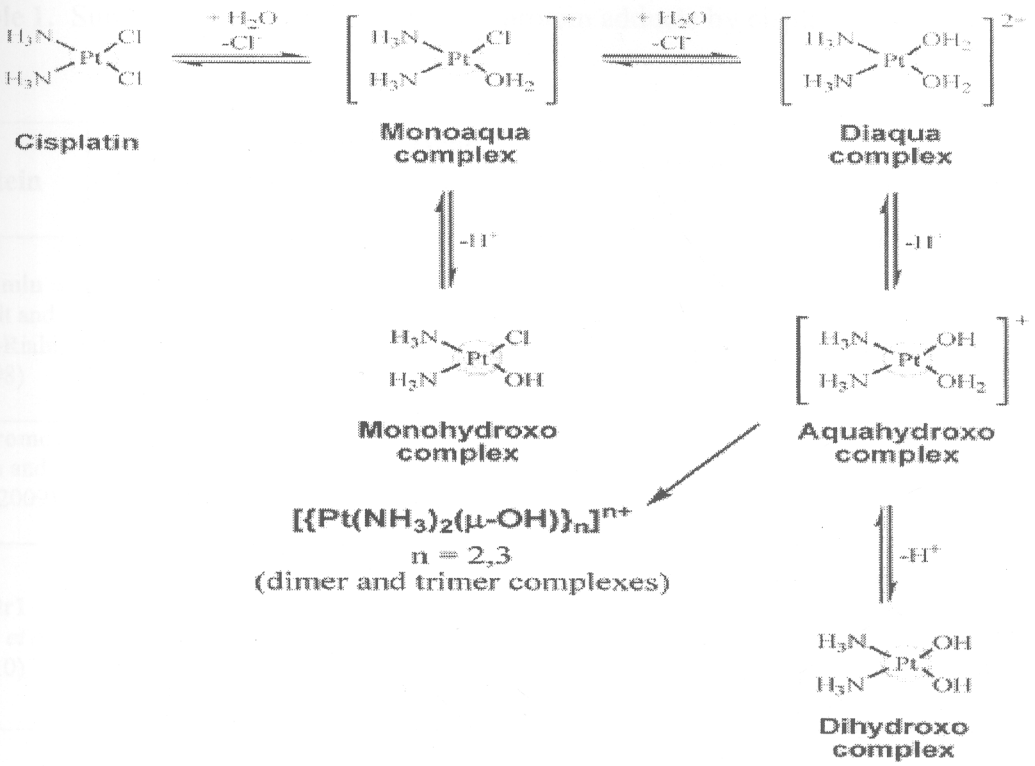

Figure 1. Chemical structure of cisplatin and its hydration [1].

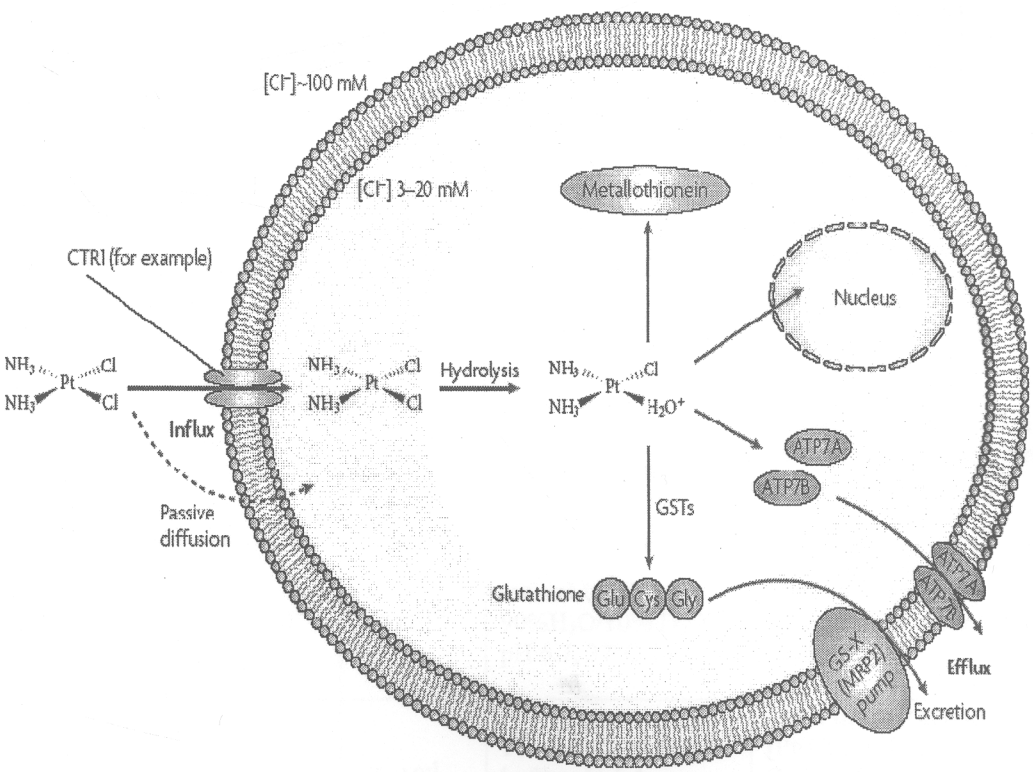

Figure 2. Cellular activation of cisplatin [2].

Table 1. Summary of the consequences of protein adducts by cisplatin.

Protein	Method	Protein conc. (M)	Drug conc. (M)	Incubation condition	Consequences
Albumin (Neault and Tajmir-Riahi, 1998)	UV-vis FT-IR	$3x10^{-4}$	$1x10^{-7}$ - $1x10^{-4}$	phosphate buffer pH 6.8-7.4, 25 mM NaCl, 37°C 2 h	- binding constant $8.52x10^{2}$ M^{-1} - secondary structural changes
cytochrome *c* (Zhao and King, 2009)	ESI-MS	$1x10^{-4}$	$4x10^{-4}$ - $1.6x10^{-3}$	5 mM NH_4OAc pH 6.8, 37°C 24 h	- monoadduct at Met 65
hCtr1 (Crider *et al.*, 2010)	LC-MS	$8x10^{-4}$	$8x10^{-4}$	23.8 mM carbonate, 100 mM NaCl, 1.13 mM phosphate pH 7.4, 37°C 24 h	- intramolecular crosslinks through replacing of all platinum ligands by three Mets and an amide nitrogen of peptide backbone
Lysozyme (Casini *et al.*, 2007)	ESI-MS X-ray crystallo-graphy	$1x10^{-4}$	$3x10^{-4}$	25 mM ammonium carbonate pH 7.4, 37°C 72 h	- monofunctional adduct at His 15
Hsp90 (Ishidaa *et al.*, 2008)	CD UV-vis	$5x10^{-8}$ - $1.1x10^{-6}$	$11x10^{-6}$ - $2x10^{-3}$	50 mM HEPES pH 7.4, 25°C	- dimer formation, - inhibited aggregation prevention of HSP90C, - altered secondary structure of HSP90N, - increased protease resistance of HSP90N
Globulin (Chen *et al.*, 1994)	gel filtration-photometry	$1.9x10^{-5}$	$1x10^{-1}$ - 1.4	50 mM phosphate buffer, 100 mM NaCl pH 7.4, 37°C 14 d	- 12.4 mol platinum per a protein (30-fold excess of cisplatin) - protein precipitation
Na,K-ATPase (Neault *et al.*, 2001)	UV-vis FT-IR	$1x10^{-4}$ – $1x10^{-3}$	$1x10^{-7}$ - $1x10^{-3}$	25 mM Tris pH 7.5, 100 mM NaCl, 2 mM $MgCl_2$, 2 mM ATP, 1 mM ouabain, 37°C 2 h	- binding constant $1.93x10^{4}$ M^{-1} - secondary structural changes
Transferrin (Cox *et al.*, 1999)	^{13}C, ^{15}N NMR	$3x10^{-4}$	$3x10^{-4}$	100 mM KCl, 90%H_2O/10% D_2O pH 6.7, 37°C 24 h	- monofunctional adduct at Met256 or Met499 - unaffected conformational change
Ubiquitin (Casini *et al.*, 2009)	ESI-MS	$1x10^{-3}$ – $2x10^{-3}$	$1x10^{-3}$ - $2x10^{-3}$	10 mM phosphate buffer pH 6.4, 37°C 24 h	- four distinct adducts: $[Pt(Ub)(NH_3)_2Cl]$, $[Pt(Ub)(NH_3)_2H_2O]$, $[Pt(Ub)(NH_3)_2]$, and $[Pt(Ub)(NH_3)]$

For instance, cisplatin can cause the structural perturbation of a synthetic peptide containing a Zn^{2+} finger domain. The platinum coordination to Zn^{2+}-binding sites resulted in Zn^{2+} ejection and subsequently loss of protein tertiary structure, implying the inhibition of critically biological functions regulated by Zn^{2+} finger protein. Such a mechanism has been discussed in the apoptosis process mediated by the interaction of cisplatin and platinum-based compounds with Zn^{2+} finger transcriptional factors [16]. Likewise, the nucleocapsid Zn^{2+} finger NCp7 protein, a protein required for the recognition and packaging of viral RNA, was attracted by some platinum compounds thereby inhibiting its nucleic acid binding and preventing the viral infectivity [17-19]. The Zn^{2+} finger protein, therefore, is a potential target for platinum compounds in medicinal application.

The breast cancer suppressor protein 1 (BRCA1) has been shown to play a vital role in genomic integrity maintenance through multiple functions in DNA damage repair, cell cycle checkpoint, protein ubiquitination and transcriptional regulation [20-22]. It contains 1863 amino acid residues that are characterized into 3 major domains, including the N-terminal Zn^{2+} finger RING domain (BRCA1 RING domain), the large central segment, and the BRCA1 C-terminal domain (BRCT) (Fig. 3).

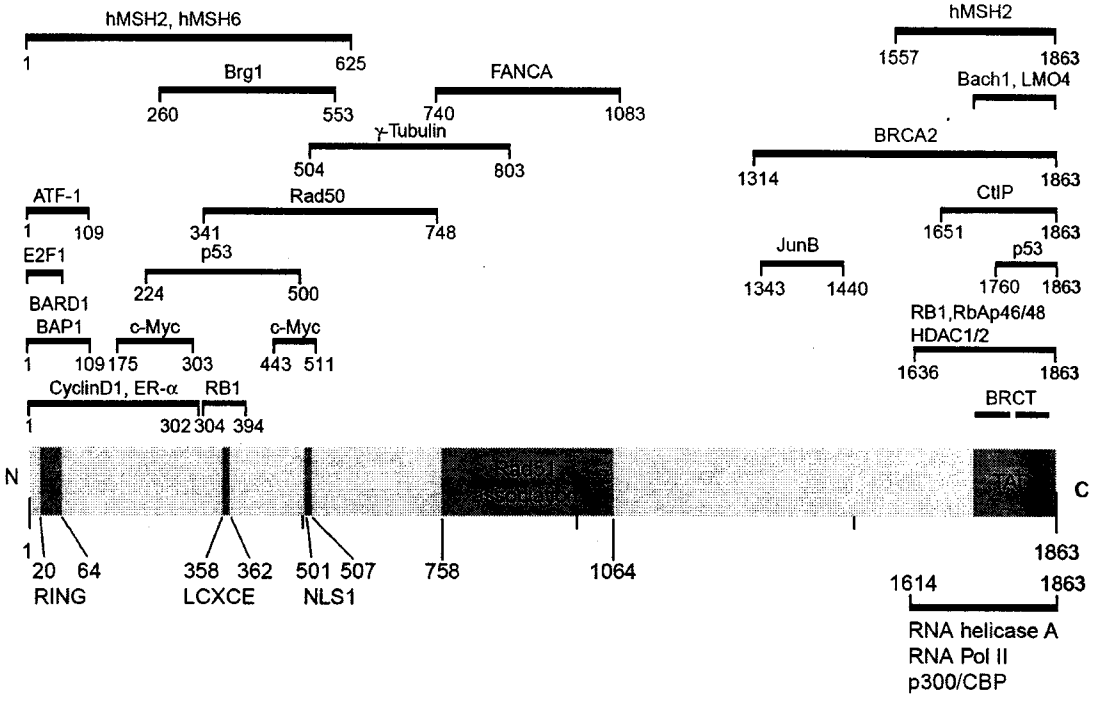

Figure 3. Schematic diagram of BRCA1 and its binding partners [20].

The BRCA1 RING domain contains the conservative sequences of cysteine and histidine (C_3HC_4) necessary for the specific coordination with two Zn^{2+} ions. Atomic structure of the BRCA1 RING domain have revealed that both ends of the domain are antiparallel α-helices, flanking the central RING motif characterized by a short antiparallel three-stranded β-sheets, two large Zn^{2+}-binding loops and a central α-helix (Fig. 4)[23]. These two metal-binding sites are established in an interleaved fashion, which the first and third pairs of cysteines (Cys24, Cys27, Cys44 and Cys47) form site I and the second and fourth pairs of cysteines and histidine (Cys39, His41, Cys61 and Cys64) form site II. It is an important domain since it can play a central role in BRCA1-mediated macromolecular interactions to exert its functions [24-25].

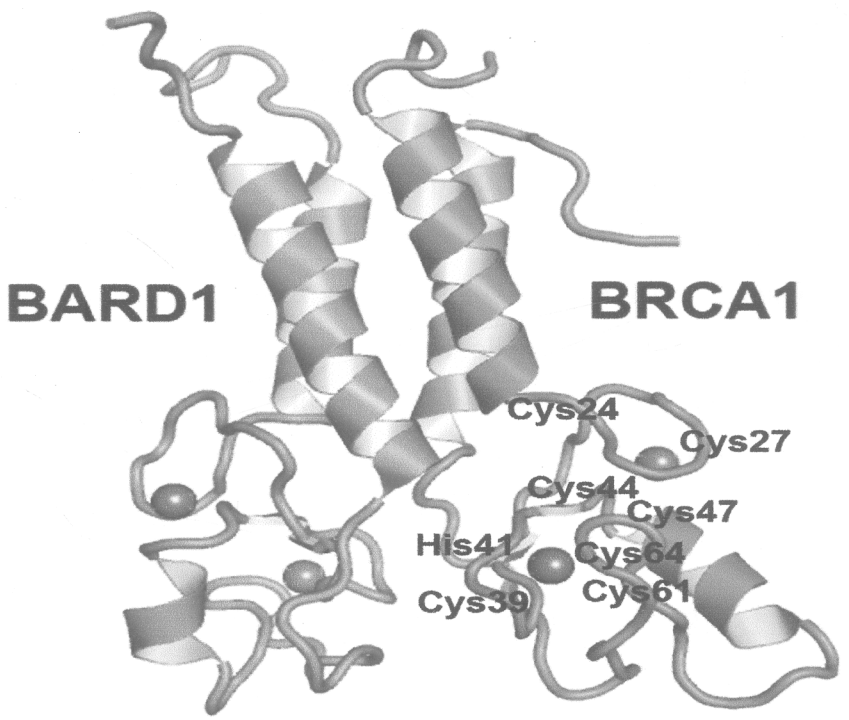

Figure 4. Solution structure of the BRCA1-BARD1 RING heterodimer. The BRCA1 subunit is shown in red, and the BARD1 subunit in blue. The grey spheres represent Zn^{2+} atoms. The dimerization interface is formed by the antiparallel α-helices, flanking the central RING motif of both BRCA1 and BARD1. The BRCA1 RING domain contains two Zn^{2+}-binding sites in an interleaved fashion, which the first and third pairs of cysteines (Cys24, Cys27, Cys44, and Cys47) form site I, and the second and fourth pairs of cysteines and histidine (Cys39, His41, Cys61, and Cys64) form site II. This structure was generated with PyMOL software (http://pymol.sourceforge.net) based on the protein databank (PDB: 1JM7) [23].

Recently, a new approach for cancer therapy is mediated by alteration in DNA repair process [26-28]. The cells with dysfunctional DNA repair accumulate the high level of DNA damage, eventually resulting in major genomic instability and cell death. Several lines of evidences demonstrated that cancerous cells with BRCA1 inactivation had a defect in DNA repair of double strand breaks (DSB) through the mechanism of homologous recombination [29-31]. The DNA cross-linking agents that generate DSBs and require the homology-directed repair would be beneficial for treatment of such cancer cells. BRCA1-deficient cells which impaired the BRCA1 function were shown to be hypersensitive to cisplatin, mitomycin C and cyclophosphamide and displayed the effectively clinical response for fighting BRCA1-associated breast and ovarian cancers or even its aggressive forms of basal-like and triple negative subtypes [32-34]. A clinical study assessed ten patients with BRCA1-positive breast cancer who were treated with cisplatin. An impressively pathologic complete response of 90% was observed in nine patients with excellent compliance [35-36]. Reconstitution of BRCA1 in the cells via transfection undoubtedly gained the BRCA1 functions and resulted in a reduced level of cancer cell death, following treatment with cisplatin or other DNA damaging agents [37]. Moreover, recent evidences revealed the implication of BRCA1 in cisplatin-resistant breast and ovarian cancer cell lines. These cells acquired resistance to DNA damaging agents mediated by secondary mutation in BRCA1. This mutation restored BRCA1 protein expression and function in DNA repair, causing the cancer cells to become more tolerant to cisplatin [38-39].

The above data demonstrated the utilization of BRCA1 dysfunction as a clinically validated target for therapeutic application [40-47]. The interaction of cisplatin with the BRCA1 protein, particularly the BRCA1 RING domain is of great interest. Alterations in Zn^{2+} coordination sites or some residues of the BRCA1 RING domain have been shown to perturb protein structure and ubiquitin ligase activity [48-50]. Therefore, targeting the BRCA1 RING domain through the disruption of Zn^{2+} coordination sites by the platinum-based drugs might be effective for the eradication of cancers and recurrently platinum-resistant cancer with lesser adverse effects than the empirical and historical treatment. In the present study, we described the first evidence for a direct binding of the anticancer drug cisplatin to the BRCA1 RING domain, particularly its conformation and thermal denaturation.

MATERIALS AND METHODS

Materials

cis-Diamminedichloroplatinum(II) (cisplatin), bovine serum albumin (BSA), isopropyl-β-D-thiogalactoside (IPTG), iodoacetamide, sodium cacodylate trihydrate, *t*-octylphenoxypolyethoxyethanol (triton X-100), phenylmethylsulphonylfluoride (PMSF) and glutaraldehyde were purchased from *Sigma Chemicals Co.* Agarose power, tris(hydroxymethyl)aminometane (molecular biology grade), elastase and trypsin (sequencing grade) and dATP, dCTP, dGTP and dTTP were from *Promega Corporation* (USA). Restriction enzymes *BamH* I and *Xho* I were obtained from *New England BioLabs Inc.* Nonidet P-40 (NP40) was purchased from *Bio Basic Inc.* Acetonitrile (HPLC grade) and kanamycin were obtained from *Roth.* Bacto™ tryptone, Bacto™ yeast extract and Bacto™ agar were from *Becton, Dickson and company.* Dithiothreitol, ethylenediaminetetraacetic acid disodium salt (EDTA), guanidine hydrochloride, trifluoroacetic acid and zinc(II) chloride were obtained from *Fluka.*

Methods

1. Preparation of the complementary DNA fragments of the *BRCA1* gene (GenBank no. U14860)

1.1 Total RNA isolation

Total RNA from human leukocytes was isolated using QIAamp® RNA Blood Kit (QIAGEN) by mixing 1 volume (1.5 ml) of the whole human blood with 5 volumes (7.5ml) of the hypotonic solution for erythrocyte lysis. The mixture was vortexed briefly 2 times during incubation on ice for 10-15 min, and subsequently centrifuged at 400xg for 10 min at 4°C. After the supernatant was discarded, the cell pellet mainly containing leukocytes was resuspended with the hypotonic solution (3 ml per 1.5 ml of the whole blood), and centrifuged at 400xg for 10 min at 4°C for complete removal of erythrocytes. The pelleted leukocytes was resuspended with the leukocyte lysis buffer (600 μl), and loaded onto the QIAshredder spin column for efficient disruption of the cells and homogenization of the lysate, resulting in the optimal yield and purity. The QIAshredder spin column was centrifuged for 2 min at

maximum speed to homogenize. The homogenized lysate was mixed with 70% ethanol (600 µl), and transferred to the QIAamp spin column, which allows RNAs longer than 200 bases to bind to the membrane. Small RNAs such as 5.8S RNA, 5S RNA, and tRNA (approximately 160, 120, and 70-90 nucleotides in length, respectively) do not bind in quantity under the conditions used. The QIAamp spin column was centrifuged at ≥ 8000xg for 15 s, and transferred into a new 2-ml collection tube. The QIAamp spin column was applied with the washing buffer 1, and centrifuged at ≥ 8000xg for 15 s to wash the RNA sample. The QIAamp spin column was placed in a new 2-ml collection tube, added with the washing buffer 2 (500 µl), and centrifuged at ≥ 8000xg for 15 s. After the flow-through was discarded, the washing buffer 2 (500 µl) was added on the QIAamp spin column, and the column was centrifuged at full speed for 3 min. RNase-free water (50 µl) was directly added onto the membrane of the QIAamp spin column, sitting in a new 1.5-ml microcentrifuge tube, and finally centrifuged at ≥8000xg for 1 min to elute total RNA.

1.2 Reverse transcriptase-polymerase chain reaction (RT-PCR)

The isolated total RNA was used as the template for complementary DNA (cDNA) synthesis, using QIAGEN OneStep RT-PCR Kit®. The combination of the Omniscript and Sensiscript reverse transcriptases was included in the enzyme mix, which provides the highly efficient and specific reverse transcription for the first strand cDNA synthesis from RNA templates with as little amount as 1 pg. The second strand cDNA synthesis was obtained by the function of HotStarTaq DNA polymerase. The reactions were heated at 95°C for 15 min to activate the DNA polymerase, and simultaneously to inactivate the reverse transcriptase. The reaction mixture was prepared by mixing template RNA (<2 µg/reaction), gene-specific primers for the cDNA synthesis of the *BRCA1* gene fragment, dNTP mix, QIAGEN OneStep RT-PCR buffer, and QIAGEN OneStep RT-PCR enzyme (Table 2). Reactions were performed on a thermal cycler, according to the thermal cycling conditions (Table 3).

Table 2. Reaction components for the One-step RT-PCR.

Components	Volume (µl)	Final concentration
RNase-free water	27	-
5x QIAGEN One-step RT-PCR buffer	10	1x
dNTP mix (10 mM of each dNTP)	2	400 µM of each
10 µM forward primer	3	0.6 µM
10 µM reverse primer	3	0.6 µM
QIAGEN One-step RT-PCR enzyme mix	2	-
Template RNA	3	1 pg -2 µg / reaction
Total volume	50	-

Table 3. Thermal cycling conditions for the One-step RT-PCR.

Reverse transcription	50°C, 30 min
Initial PCR activation	95°C, 15 min
3-step cycling	
denaturation	94°C, 30 s
annealing	55°C, 45 s
extension	72°C, 1 min
Number of cycles	30 cycles
Final extension	72°C, 10 min

1.3 DNA amplification of the *BRCA1* gene fragment

The *BRCA1* gene fragments, containing the nucleotides 1-417, were amplified by the polymerase chain reaction (PCR) using the *BRCA1* cDNA as the templates. The reaction mixtures were prepared by mixing template DNA, primer solutions (Table 4), dNTP mix, 10X ProofStart PCR buffer, and water followed by the addition of the ProofStart DNA polymease (QIAGEN) to the individual PCR tubes. The reactions (Table 5) were performed on a thermal cycler, according to the thermal cycling conditions (Table 6). The PCR products were electrophoresed on 1% agarose gel, and then extracted by QIAquick® gel extraction kit (QIAGEN).

Table 4. The oligonucleotide primers for the amplification of the *BRCA1* gene fragment

Construct name	Protein residue	Primer	Direction (5′ → 3′)
BRCA1 (1-139-wt)	1-139	forward	GACACGCGGATCCATGGATTTATCTGCTCTTCG
		reverse	GACACCGCTCGAGTCACTGTAGAAGTCTTTTGGCAC

Table 5. Reaction components for PCR amplification.

Components	Volume (μl)	Final concentration
Double distilled water	variable	-
10X ProofStart PCR buffer	10	1x
dNTP mix (10 mM of each dNTP)	3	300 μM of each
10 μM forward primer	10	1 μM
10 μM reverse primer	10	1 μM
ProofStart DNA polymerase	2	5 units
Template DNA	variable	100 ng - 1 μg / reacion
Total volume	100	-

Table 6. Thermal cycling conditions for PCR.

Initial denauration	95°C, 5 min
3-step cycling	
denaturation	95°C, 30 s
annealing	55-63°C, 45 s
extension	72°C, 1 min
Number of cycles	35 cycles
Final extension	72°C, 10 min

1.4 Extraction and purification of the PCR products

The PCR products from 1.3 were electrophoresed on 1% agarose gel. DNA fragments were detected by staining with ethidium bromide, and visualizing by illumination with 300 nm UV light. Targeted DNA fragments were sliced from the agarose gel with a clean and sharp scalpel, and extracted by QIAquick® gel extraction kit (QIAGEN). Three volumes of the solubilizing buffer were added to a volume of

gel (100 mg ~ 100 µl) to dissolve the agarose gel slice, and to provide the appropriate conditions (high salt and pH ≤ 7.5) for binding of DNA to the silica gel membrane while the contaminants pass through the column. The mixture was incubated at 50°C for 10 min, then loaded onto a QIAquick spin column, and centrifuged at 10000xg for 1 min. The flow-through was discarded, and the washing buffer (750 µl) was added to the QIAquick spin column that was subsequently centrifuged at 10000xg for 1 min. The flow-through was discarded, and the QIAquick spin column was additionally centrifuged at 10000xg for 1 min to completely eliminate the washing buffer. Water (50 µl) was directly added onto the membrane of the QIAquick spin column, sitting in a new 1.5-ml microcentrifuge tube, and finally centrifuged at full speed for 1 min to elute purified DNA.

2. Plasmid constructions

The short N-terminal fragment of the BRCA1 protein amino acid residues 1-139 was produced as the intact protein by inserting the respective gene fragment (the *BRCA1* gene nucleotides 1-417) into the *Bam*HI/*Xho*I sites of a bacterial plasmid pET28a(+) derivative (Fig. 5). The digestion reactions (50 µl) contained 5 µl of 10x enzyme buffer, 0.5 µl of 100x BSA, DNA fragments or 10 µg of plasmids (pET28a(+) derivatives), 1 µl of each endonuclease (20 units), and water. The reactions were then incubated at 37°C for 6 h, and subsequently electrophoresed on 1% agarose gel. The digested DNA fragments were purified using QIAquick® gel extraction kit. The digested DNA fragments were ligated into the respective endonuclease sites of the plasmids by T4 DNA ligase. The ligated constructs were transformed to *E. coli* DH5α by mixing the ligation reactions with 100 µl of competent cells, and then the cells were incubated on ice for 30 min. The cells were shocked at 42°C for 90 s, and immediately placed on ice for 5 min. LB broth (800 µl) was added to the cells, and further incubated at 37°C for 1 h. The cells were centrifuged at 5000xg for 1 min. The medium was discarded, and the cell pellet was resuspended in 100 µl of the fresh LB broth. The cells were grown on LB agar, containing kanamycin (30µg/ml). The recombinant plasmids were isolated, and characterized by restriction analysis and DNA sequencing.

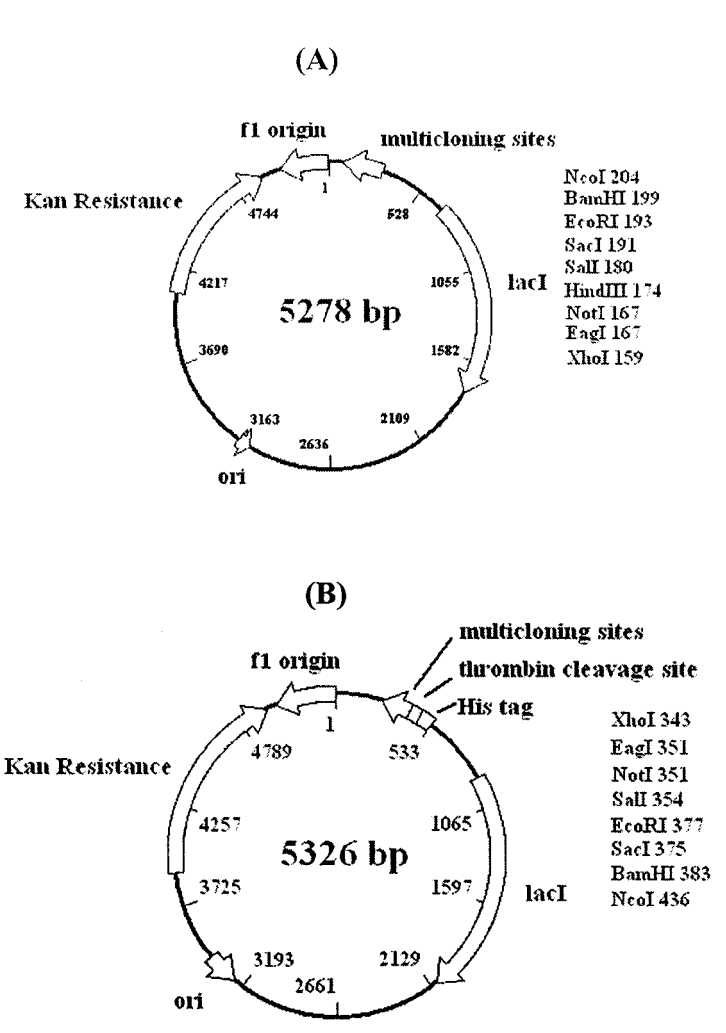

Figure 5. Schematic representations of the bacterial expression plasmids. (A) pET28a(+) derivative without the His_6 fusion tag, and (B) pET28a(+) derivatives with the His_6 fusion tag.

3. Verification of the recombinant plasmids by automated DNA sequencing

The inserted *BRCA1* fragment was verified by DNA sequencing using Big Dye Terminator Cycle Sequencing Ready Reaction Kit (Applied Biosystem, Foster City). The reaction mixtures consisted of Big dye Terminator ready reaction mix (8 µl), double strand DNA template (200-500 ng), and primer (3.2 pmol) in 20 µl of total volume, and were placed in a thermal cycler, and run for 25 cycles of 96°C for 10 s, 50°C for 5 s, and 60°C for 4 min with an initial denaturation at 96°C for 1 min. The unincorporated Big Dye Terminator was removed by the addition of 75% isopropanol (80 µl) that was subsequently left at room temperature for 15 min. The mixtures were spun at 14000xg for 20 min at room temperature, and the supernatant was discarded.

Ethanol (70%) (250 μl) was added, and the samples were spun at 14000xg for 5 min. After the supernatant was discarded, the samples were dried in a heat-block at 90°C for 1 min. The samples were resuspended in 6 μl of the loading dye (deionized formamide and Blue dextran at the ratio of 1:5), heated at 90°C for 2 min, and then placed on ice immediately. One microliter of each sample was loaded into a separate lane of polyacrylamide gel, and run in a DNA sequencer. The sequence data were aligned to *BRCA1* (GenBank no. U14860) databases.

4. Expression and purification of the recombinant proteins

All recombinant plasmids were transformed into *E. coli* BL21(DE3) for productions of the proteins. Transformed bacterial cells were grown in 1000 ml of Luria Broth medium with 30 μg/ml kanamycin at 37°C. Isopropyl-β-D-thiogalactoside was added to a final concentration of 0.5 mM to induce the expression, when the $A_{600\ nm}$ reached 0.5-0.6. Cells were allowed to grow for 4 h after induction and harvested by centrifugation. Cell pellets were resuspended in 20 ml of lysis buffer [50 mM Tris (pH 7.6), 50 mM NaCl, 10 mM DTT, 1% Triton X-100, 0.5% NP-40, and 1 mM PMSF] and then lysed with a French press. Lysate was centrifuged at 13,000xg at 4°C for 30 min. The intact BRCA1 proteins (amino acid residues 1-139) were accumulated in the inclusion bodies. They were washed with 30 ml of lysis buffer, and subsequently centrifuged at 13,000xg at 4°C for 30 min. The inclusion bodies were solubilized with 30 ml of 6 M guanidine HCl in 50 mM Tris (pH 7.4), and 10 mM β-merceptoethanol at room temperature for 3 h with stirring. The mixtures were centrifuged at 13000xg for 30 min at 10°C, and the supernatant was dialyzed overnight at 4°C against 0.1% acetic acid. The mixtures were then centrifuged at 13000xg for 30 min at 4°C, and the resulting supernatant was filtered through a 0.2 μm cellulose acetate membrane. The filtrates were further purified using an analytical C4 reversed-phase column (Vydac protein C4 column; 4.6/250 mm dimensions with 5 μm particle size) with a water/acetonitrile (ACN) gradient containing 0.1% trifluoroacetic acid. Protein solutions were eluted with a linear 40-60% ACN gradient at a rate of 0.35%/min. Purified protein was identified on 15% Coomassie blue-stained SDS-PAGE, and subsequently confirmed by sequencing the tryptic digested peptides. The amount of proteins was quantitated by the Bradford assay using BSA as standard.

5. Gel-filtration chromatography

Purified BRCA1(1-139) proteins from reversed-phase chromatography were lyophilized, and resuspended in 2 M guanidine HCl with three molar equivalent ratio of Zn^{2+} to protein. Proteins (0.3 mM) were then applied on an analytical Superose 12 HR 10/30 column (Amersham Biosciences) using the 200 μl of sample loop, and the flow rate of 0.4 ml/min. The column was pre-equilibrated with 25 mM Tris (pH 7.0), 150 mM NaCl, and 10 μM $ZnCl_2$, and calibrated using BSA (67 kDa), ovalbumin (45 kDa), chymotrypsinogen A (25 kDa), and ribonuclease A (13.7 kDa). The elution profiles were monitored at 212 nm.

6. Glutaraldehyde cross-linking

Peak fractions from gel filtration column (typically 2 μM) were subjected to the cross-linking reaction in the presence of 0.001-0.05% glutaraldehyde (w/v) at ambient temperature. Reaction aliquots (20 μl) were removed at 0, 15, 30, and 60 min after the addition of glutaraldehyde, quenched with an equal volume of SDS-loading dye, and then heated at 95°C for 5 min. The reactions were visualized on 15% SDS-PAGE by silver staining.

7. Limited proteolysis and mass spectrometry

Protein samples (30 μM) in the absence and presence of 3 mol-equiv. ratio of Zn^{2+} to protein were prepared in 10 mM cacodylate buffer pH 6.8 and mixed with either elastase or trypsin at the protein/protease ratio of 100-500:1 (w/w) at 37°C. Reaction aliquots at different time intervals (0, 0.25, 0.5, 1, 2, 3, 6, 12, and 24 h after the addition of protease) were quenched by adding an equal volume of SDS-loading dye. Samples were visualized on 15% SDS-PAGE by Coomassie blue staining. Proteolysis of metal-free protein was also determined in the presence of 0.5 mM EDTA. To determine the constituents of the digested products, the protein bands of interest from the SDS-PAGE gel were excised, in-gel alkylated with iodoacetamide, and digested with sequencing-grade trypsin (Promega). In-gel digestions of free BRCA1 and cisplatin-BRCA1 adducts for characterizing the binding sites of cisplatin were also performed with ignoring the modification by iodoacetamide. The peptide mixture was separated on a PepMap C18 column (75 μm/150 mm dimensions with 3 μm particle size) that connected to an UltiMate 3000 HPLC system (Dionex, Idstein,

Germany), using a gradient of 4-50% acetonitrile. Eluted peptides were ionized by electrospray ionization (ESI), and mass spectra were acquired with a QTRAP 4000 Mass Spectrometer (Applied Biosystems/MDS Sciex). MS/MS Analyses were conducted using collision-energy profiles chosen on the basis of the m/z value and the charge state of the parent ion. The Analyst/Bioanalyst software (version 1.4.1, Applied Biosystems) was used to process and submit the data to the MASCOT server (version 2.2, Matrix Science Ltd., London, UK) for in-house search against the SwissProt protein database. The mass tolerance of precursor ions and sequence ions was set to 0.4 Da. The searches included variable modifications of cysteine with propionamide and carbamidomethyl, and methionine oxidation.

8. Circular dichroism

Protein samples (10 μM) were prepared in 10 mM cacodylate buffer pH 6.8, according to Bradford assay using BSA as standard. $ZnCl_2$ and cisplatin were prepared as 5 mM stock solutions in deionized water. Metal-dependent folding of the protein was monitored by acquiring CD spectra over a range of 200-260 nm using a Jasco J720 spectropolarimeter (Japan Spectroscopic Co. Ltd., Hachioji City, Japan) with a programable Peltier type cell holder that allows for the temperature control. Measurements of Zn^{2+} and cisplatin binding were carried out at 20°C using a 0.1 cm quartz cuvette. The spectrum was the average of five separate spectra with a step size of 0.1 nm, a 2 s response time, and a 1-nm bandwidth. Data were baseline-corrected by the subtraction of cacodylate buffer. The secondary structures of proteins were predicted by the CONTIN program [51]. The effect of Zn^{2+} and cisplatin bindings on the protein stability was determined in the absence and presence of 3 mol-equiv. ratio of Zn^{2+} to protein. CD experiments, involving thermal denaturation, were performed in three separate scans in the range from 15°C to 95°C at 208 nm with a heat rate of 1°C/min. Thermal renaturation (20°C after being heated at 95°C) was also observed. The binding constant was determined using Eqn. 1 [52]:

$$\theta_{obs} = \theta_{max}[(1+(KC/N)+KP)/(2KP) - \sqrt{(((1+(KC/N)+KP)/(2KP))^2 - C/(NP))}] \quad (1)$$

in which θ_{obs} is the observed ellipticity change at any concentration of metal, θ_{max} is the ellipticity change, when all of the protein binds metal, K is the binding constant, P

is the protein concentration, C is the concentration of metal added, and N is the number of binding sites.

The free energy of binding was given by Eqn. 2.

$$\Delta G = -RT \ln k \qquad (2)$$

in which ΔG is the free energy, R is the gas constant of 1.987 cal mol^{-1}, T is the temperature in Kelvin, and K is the binding constant.

Expression and purification of the BRCA1 RING domain

The BRCA1 RING domain consisting of residues 1-139 was expressed in *E. coli* BL21(DE3) with the regulation of the inducible T7 promoter of a pET28a (+) derivative. Because of the restriction sites used, BRCA1 contained the leading MGS residues derived from the plasmid. It was purified to an apparent homogeneity by reversed phase chromatography (Fig. 6). Partial amino acid sequences of BRCA1 were verified by analysing the peptides from a tryptic digestion with mass spectrometry (Fig. 7). The experimentally obtained sequences corresponded to the N-terminal region of BRCA1. Purified BRCA1 proteins were further used to characterize some properties in the following experiments.

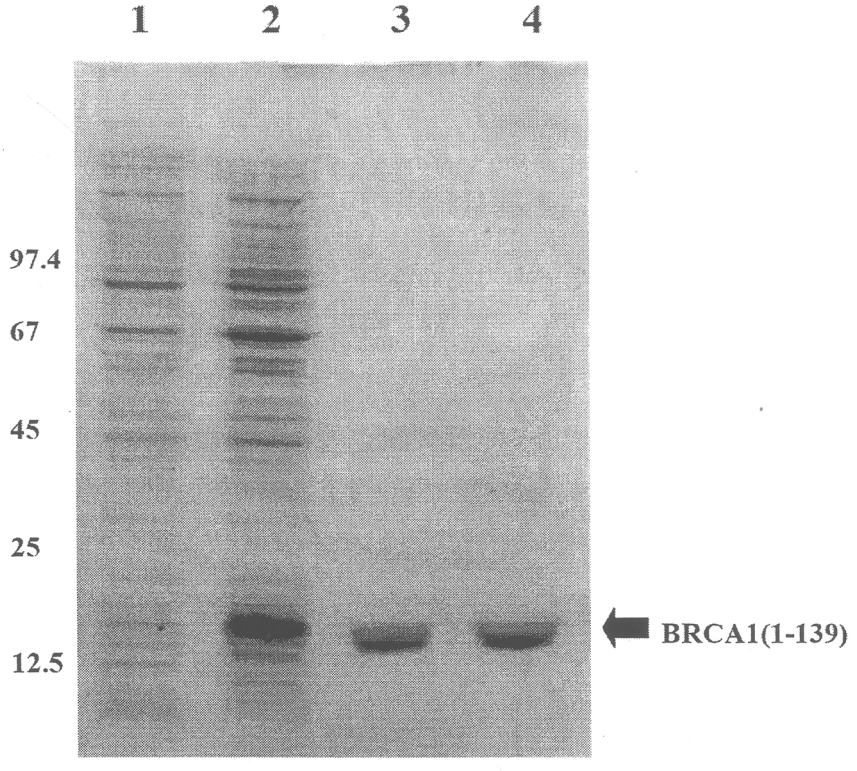

Figure 6. Expression and purification of the BRCA1 RING domain. Transformed *E. coli* BL21(DE3) cells were induced with 0.5 mM IPTG and analysed by 15% SDS-PAGE with Coomassie blue staining. Lane 1: whole-cell lysate uninduced; Lane 2: whole-cell lysate after a 4 h induction; Lane 3 and 4: purified BRCA1 protein after reversed phase chromatography. The molecular mass marker (kDa) was positioned.

```
                                  *  *                 *  *  *  *
1   MDLSALRVEE VQNVINAMQK ILECPICLEL IKEPVSTKCD HIFCKFCMLK  50

                        *  *
51  LLNQKKGPSQ CPLCKNDITK RSLQESTRFS QLVEELLKII CAFQLDTGLE 100

101 YANSYNFAKK ENNSPEHLKD EVSIIQSMGY RNRAKRLLQ           139
```

Figure 7. Amino acid sequencing of the peptides after tryptic digestion. BRCA1 protein band from Coomassie blue-stained SDS-PAGE was excised, alkylated with iodoacetamide, in-gel digested with trypsin, and then analysed by LC/ESI-MS/MS. Amino acid sequences of each tryptic peptide were indicated in italic bold letters. These corresponded to the N-terminal region of BRCA1. The Zn^{2+}-binding sites were identified with the asterisk.

Protein secondary structure

CD spectra of the BRCA1 RING domain with and without Zn^{2+} bound showed similar profiles in shape with some differences in their amplitudes (Fig. 8). This indicated the potential preformation of the BRCA1 structure in the absence of Zn^{2+} or apo-form and the BRCA1 RING domain gained additionally folded structure in the holo-form after Zn^{2+} binding. A nonlinear least-squares fit of the BRCA1-Zn^{2+} binding isotherm with a simple 1:2 coordination model yielded a binding constant of $2.79\pm0.24 \times 10^6\ M^{-1}$ and provided the free energy of binding (ΔG) of -8.64 kcal mol^{-1} (Fig. 9).

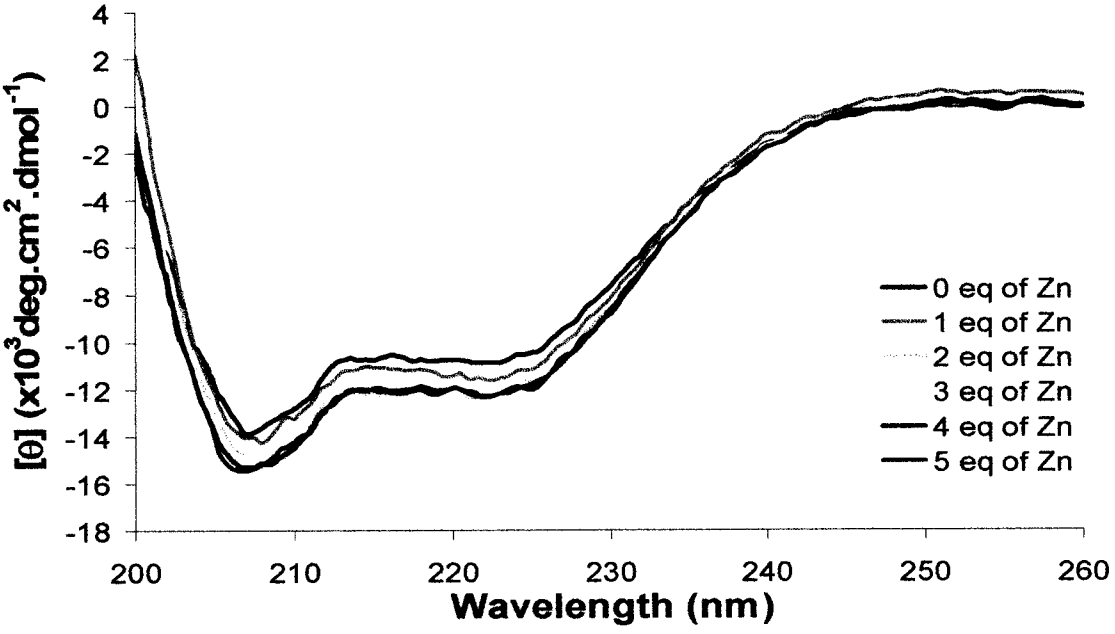

Figure 8. The CD spectra of the BRCA1 RING domain. Samples (0-5 mol- equiv. ratio of Zn^{2+} to protein) were used to monitor Zn-dependent folding property of the BRCA1 RING domain. Values were given as the mean residue ellipticity. Samples were incubated with Zn^{2+} at 4°C for 24 h before CD measurement. The measurements were performed at 20°C with the scanning rate of 50 nm/min.

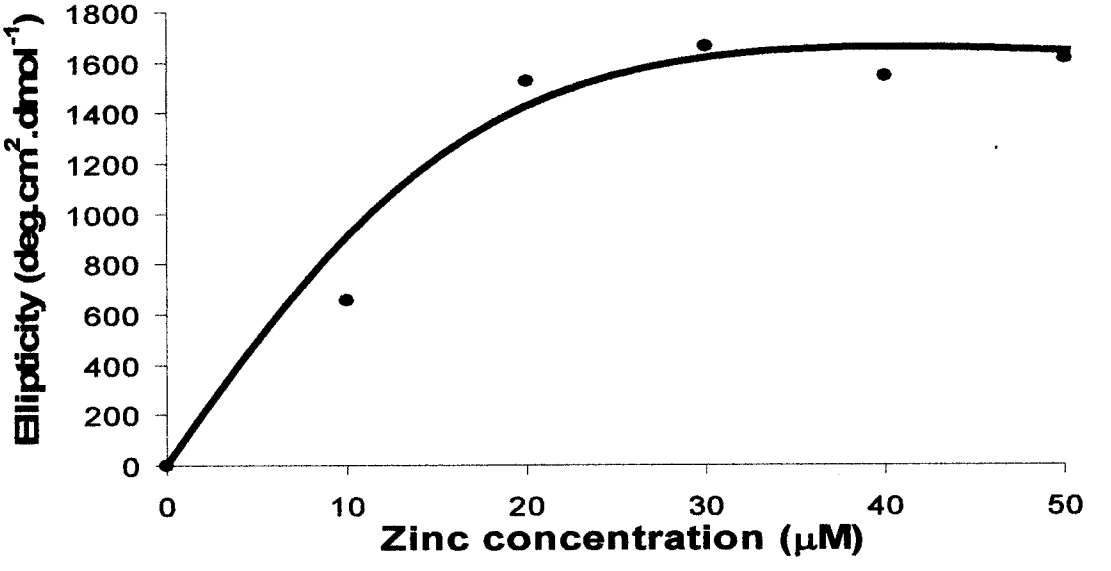

Figure 9. Titration curve of Zn^{2+} binding to BRCA1. Changes in ellipticity of protein at 208 nm with increasing Zn^{2+} concentration were plotted, and the binding constant calculated using Eqn. 1 was 2.79±0.24 x 10^6 M^{-1}.

Moreover, limited proteolysis was used to probe the structural consequence upon Zn^{2+} binding. BRCA1 without Zn^{2+} or in excess of EDTA was rapidly degraded after the addition of elastase (Fig. 10A). Two residual fragments were apparent and the examination by in-gel tryptic digestion with mass spectrometry revealed the identity of the residues 1-88 and 8-38 which possessed only the minimum RING domain. Similar results were obtained with trypsin digestion (Fig. 10B). The results suggested that BRCA1 without Zn^{2+} was considerably flexible with slightly or no protease-resistance. On the other hand, BRCA1 with Zn^{2+} was rather resistant to proteolysis throughout the course of time (Fig. 10C and 10D). It indicated that Zn^{2+} causes the structure of the BRCA1 protein to be more folded or rigid with reduced proteolytic susceptibility throughout its C-terminal portion.

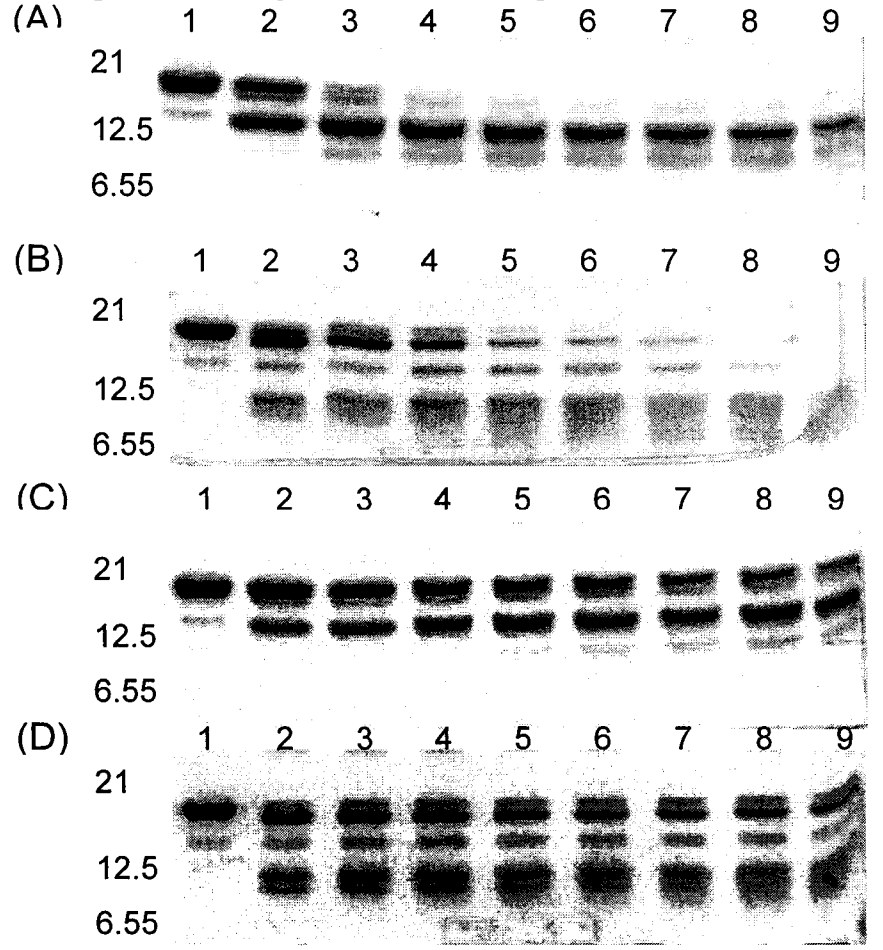

Figure 10. Limited proteolysis of the BRCA1 RING domain. Purified BRCA1 proteins without (A and B) and with (C and D) Zn^{2+} were incubated with elastase (A and C) or trypsin (B and D) at the protein/protease ratio of 100-200:1 (w/w). Reaction aliquots were removed at 0, 0.25, 0.5, 1, 2, 3, 6, 12 and 24 h after the addition of protease (Lanes 1-9, respectively) and then identified on 15% Coomassie blue-stained SDS-PAGE. The molecular mass marker (kDa) was positioned.

Cisplatin binding to BRCA1 and protein conformation

It was well established that cisplatin induced the bi-molecular protein adducts through the intermolecular crosslinks of some proteins [11]. The types of adduct formation by cisplatin are distinctive and dependent on the accessibility of platinum center and protein side-chains. The BRCA1 RING domain formed intermolecular crosslinks caused by cisplatin and the high amount of crosslinks was accompanied by an increase in cisplatin concentration (Fig. 11). This result was further verified by mass spectrometric analysis, suggesting favourably mono-molecular and bi-molecular cisplatin-BRCA1 adducts (Fig. 12).

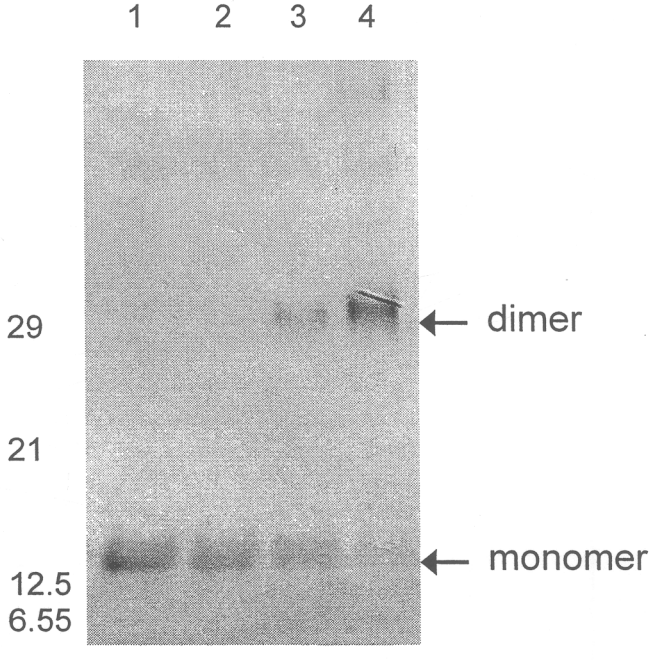

Figure 11. 15% SDS-PAGE of BRCA1 intermolecular crosslinking by cisplatin. BRCA1 proteins (10 μM) were incubated with a number of cisplatin concentrations in the dark at 37°C for 24 h. Lane 1: protein without cisplatin; Lane 2-4: proteins with 10, 100, and 1000 μM cisplatin, respectively. The molecular mass marker (kDa) was positioned.

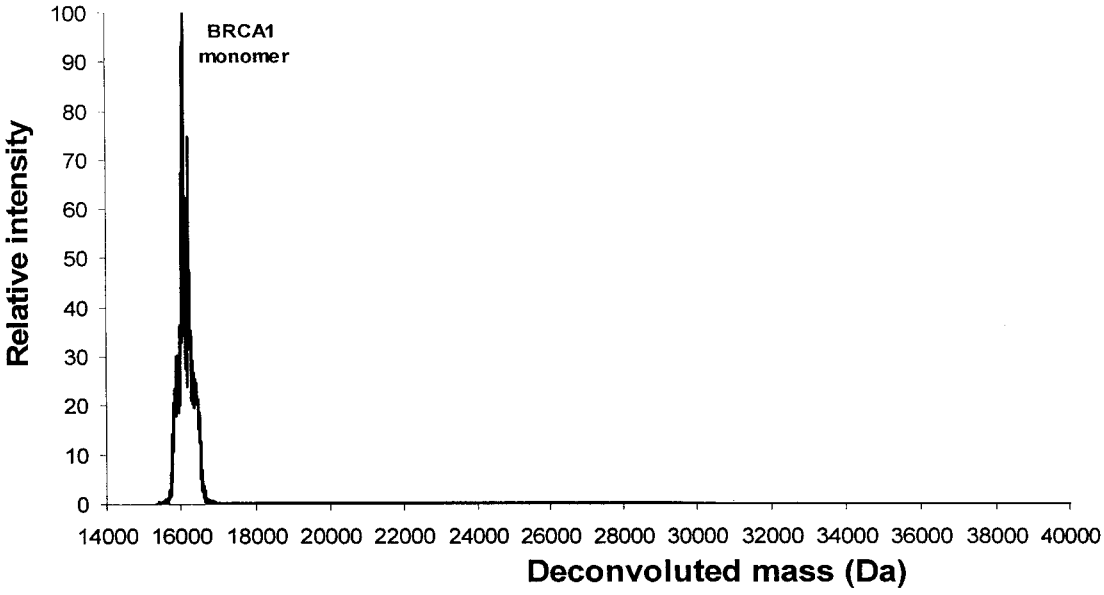

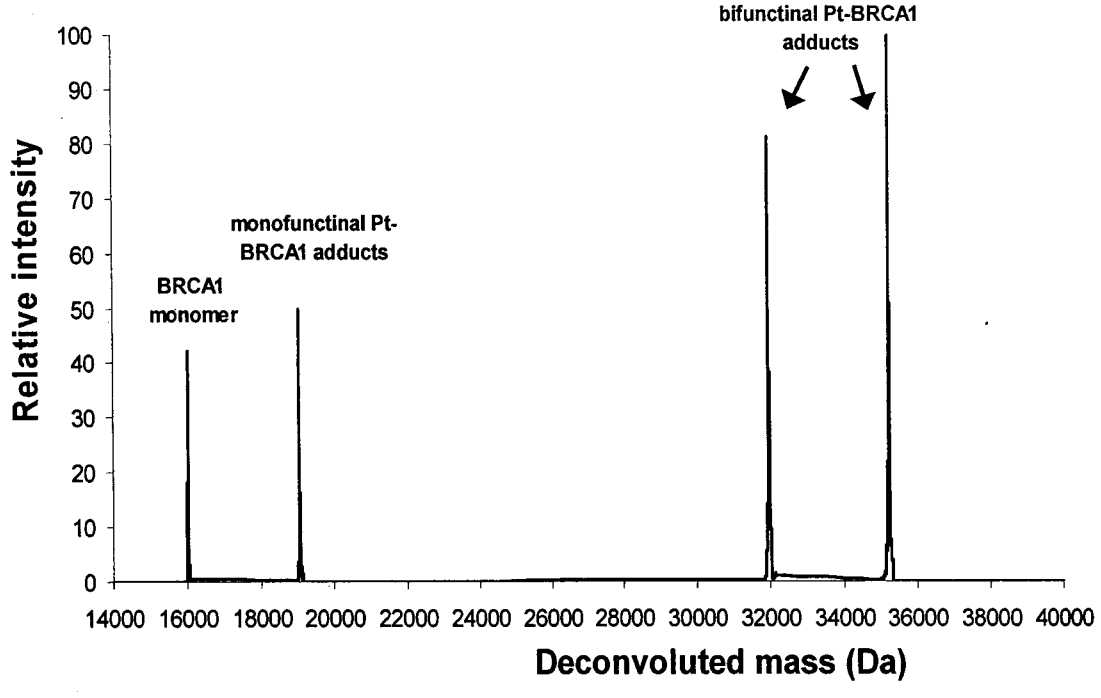

Figure 12. MS Analyses of cisplatin-BRCA1 adducts. (A) BRCA1 proteins (15 μM) or (B) cisplatin-BRCA1 adducts (1:1) were incubated in the dark at 37°C for 24 h. Samples were directly subjected to an ESI mass spectrometer, and the deconvoluted spectra were given.

Although cisplatin has been demonstrated to induce protein dimerization and perturbed some protein structures, but the secondary structure of the BRCA1 RING domain in the apo-form was maintained and underwent more folded structural rearrangement after increasing cisplatin concentrations as judged by an increase in negative CD spectra at 208 and 220 nm (Fig. 13A). It was possibly that cisplatin might bind to the unoccupied Zn^{2+}-binding sites and cause the structural changes from 50% α-helix, 9% β-sheets, 14% turn and 26% disordered element to 60% α-helix, 2% β-sheets, 15% turn and 24% disordered element, respectively. The binding constant of the in vitro platination was $3.00\pm0.11 \times 10^6\ M^{-1}$ and the free energy of binding (ΔG) was -8.68 kcal mol^{-1} (Fig. 14). In addition, CD spectra of BRCA1 pre-incubated with Zn^{2+} gave the identical profiles, suggesting that cisplatin could interact with other residues rather than the Zn^{2+}-binding sites and barely affected the overall conformation of Zn^{2+}-bound BRCA1 (Fig. 13B).

To locate the binding site of cisplatin on BRCA1, in-gel tryptic digestion of free BRCA1 and cisplatin-BRCA1 adducts (molar ratio 1:1) were subjected to LC/MS. The result revealed a unique fragment ion (+2) with a peak at m/z 656.29 obtained only from cisplatin-BRCA1 adduct digests (Fig. 15).

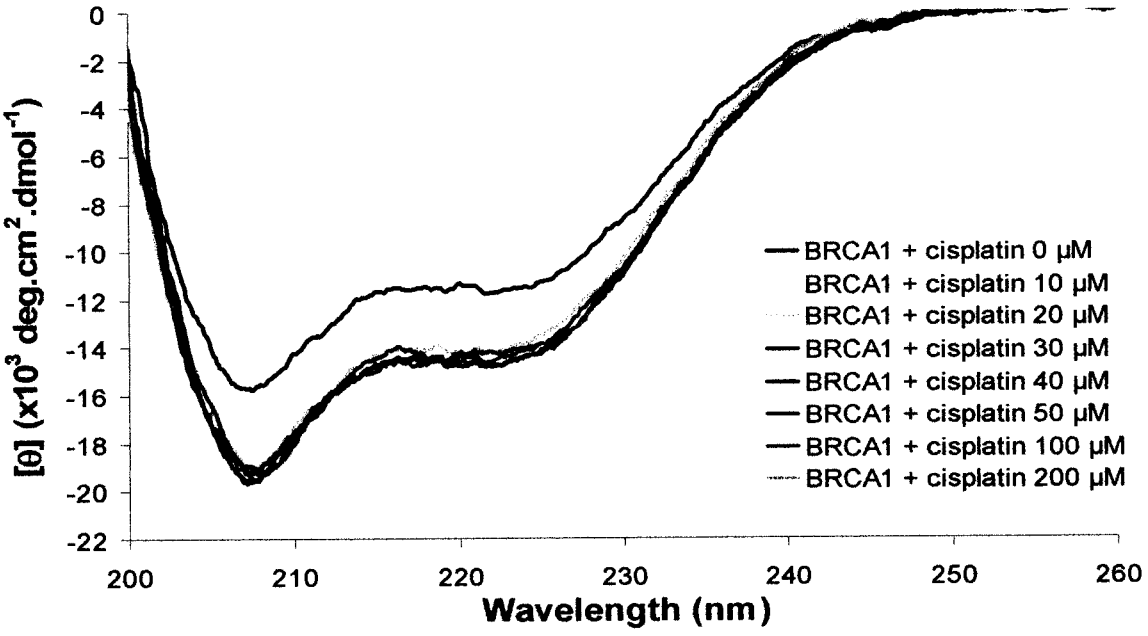

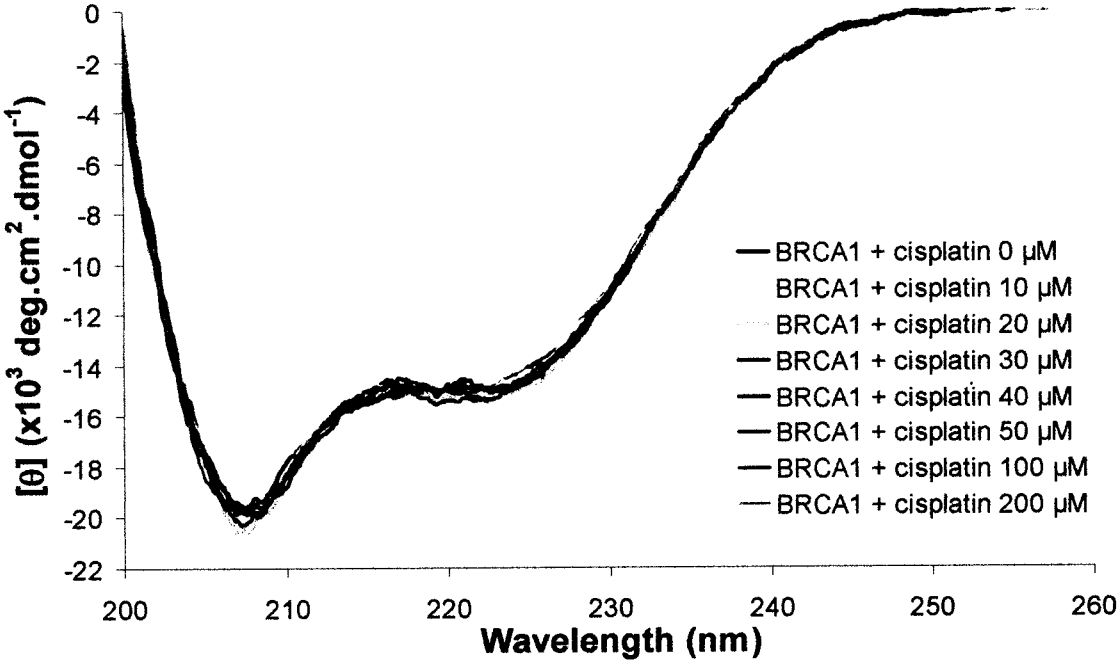

Figure 13. The CD spectra of cisplatin-BRCA1 adducts. BRCA1 proteins (10 μM) without Zn^{2+} (A) and with pre-incubation of 3 mol-equiv. ratio of Zn^{2+} to protein (B) were mixed by a number of cisplatin concentrations. Samples were incubated in the dark at ambient temperature for 24 h before CD measurement at 20°C with the scanning rate of 50 nm/min. The mean residue ellipticity and wavelength ranging from 200 to 260 nm were plotted.

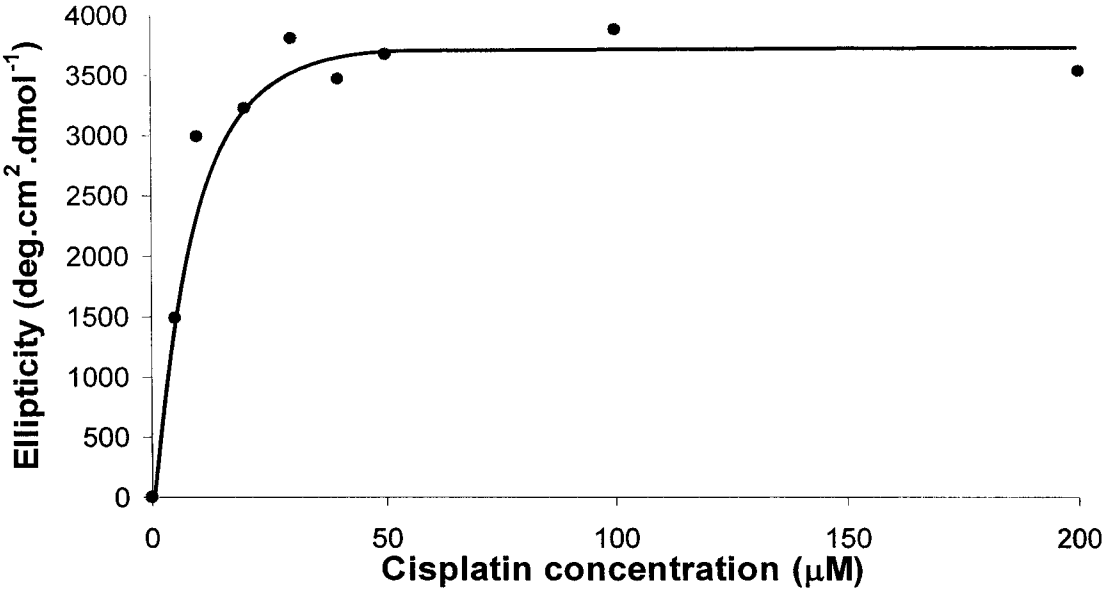

Figure 14. Titration curve of cisplatin binding to BRCA1. Changes in ellipticity of protein at 208 nm with increasing cisplatin concentration were plotted. The binding constant calculated using Eqn. 1 was 3.00±0.11 x 10^6 M^{-1}.

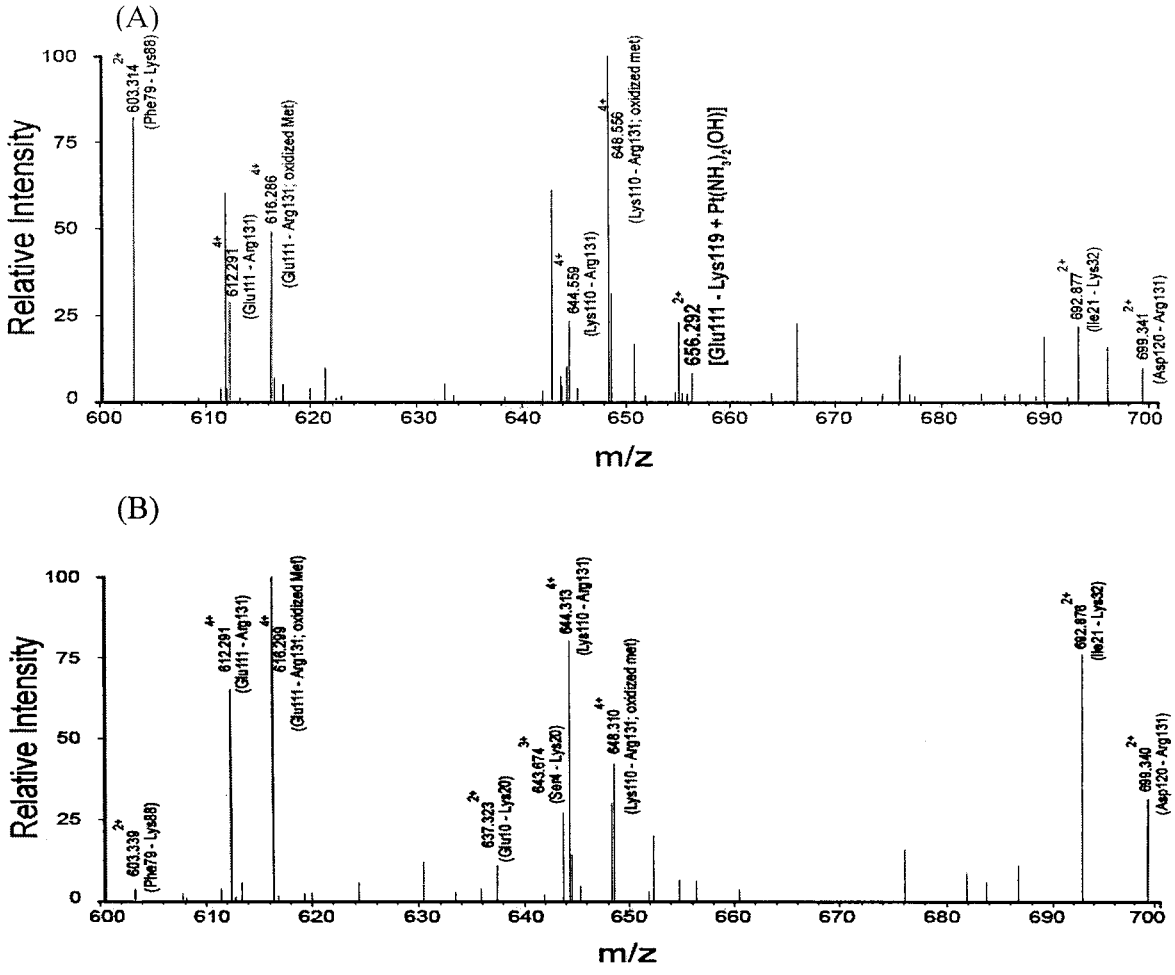

Figure 15. MS Analyses of the cisplatin-BRCA1 adduct digests. In-gel tryptic digestion of (A) the cisplatin-BRCA1 adducts (molar ratio 1:1), and (B) free BRCA1 were subjected to analysis by LC/MS. A unique fragment ion of 656.29^{2+} only derived from the cisplatin-BRCA1 adduct digests presented a Pt-containing peptide.

Tandem MS analyses (MS/MS) of the 656.29^{2+} ion (measured mass 1310.57 Da) indicated that the ion arose from $[Pt(NH_3)_2(OH)]^+$ (theoretical mass 245.99 Da) which was attached to a BRCA1 peptide ^{111}ENNSPEHLK^{119} (theoretical mass 1066.44 Da) with a mass difference of 0.86. Coordination of water to cisplatin lowers its pK_a (pK_{a1} 5.37 and pK_{a2} 7.21) to give hydroxo forms [53]. This product potentially reacted with BRCA1 and yielded BRCA1-$Pt(NH_3)_2(OH)$ as described by the following reactions.

$$Pt(NH_3)_2Cl_2 + 2H_2O \rightleftharpoons [Pt(NH_3)_2(H_2O)_2]^{2+} + 2Cl^-$$

$$[Pt(NH_3)_2(H_2O)_2]^{2+} \rightleftharpoons [Pt(NH_3)_2(H_2O)(OH)]^+ + H^+$$

$$BRCA1 + [Pt(NH_3)_2(H_2O)(OH)]^+ \rightleftharpoons BRCA1\text{-}Pt(NH_3)_2(OH) + H_3O^+$$

The product-ion spectrum of the ion (+2) with the peak at m/z 656.29 revealed the sequence ions (b_2^+, $[b_3\text{-}H_2O]^+$, $[b_4\text{-}H_2O]^+$, $[b_6\text{-}H_2O]^+$, $[b_7\text{-}H_2O]^+$, b_7^+, $[b_8\text{-}H_2O]^+$, b_8^+ and y_2^+ which corresponded to the peptide Glu111-Lys119 of BRCA1 (Fig. 16). The ions with peaks at 1165.53 and 1293.57 were the Pt-bound b_8^+ (theoretical m/z 1166.39) and b_9^+ (theoretical m/z 1294.43), respectively whereas the ion corresponding to the peak at m/z 656.28 was assigned as the Pt-free b_6^+ ion with losing a water molecule (theoretical m/z 653.26). It is speculated that cisplatin interacts with the counterpart of the b_6^+ ion (His117-Lys119). The ion with the peak at m/z 641.32 ion was the Pt-containing y_3^+ ion (theoretical m/z 642.24), and the ion with the peak at m/z 260.19 was the Pt-free y_2^+ ion (theoretical m/z 260.20). The difference in m/z (381.13 Da) indicated the binding of cisplatin to His117 (theoretical m/z 382.05 Da).

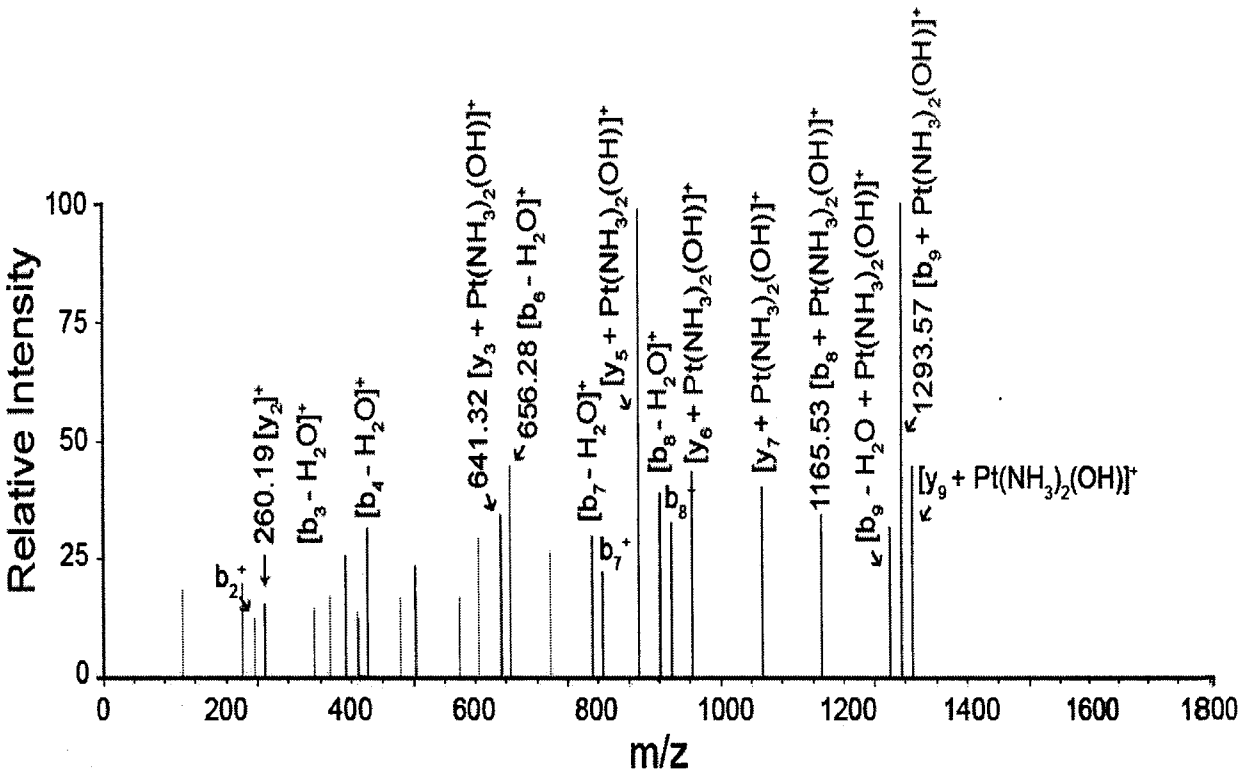

Figure 16. The product-ion spectrum of the MS/MS analysis for the 656.29^{2+} ion. It indicated that $[Pt(NH_3)_2(OH)]^+$ attached to a peptide ^{111}ENNSPEHLK^{119} of BRCA1.

Thermal denaturation of cisplatin-BRCA1 adducts

Thermal denaturation was monitored by CD to follow heat-induced unfolding which determined the effect of cisplatin binding on the stability of the BRCA1 RING domain. BRCA1 pre-incubated with or without Zn^{2+} was incubated with cisplatin and CD spectra showed the identical changes with an increase in ellipticity when the temperature was raised from 15°C to 95°C (Fig. 17). It indicated that the folded proteins gradually lost the contents of the ordered structures. When cooling to 20°C after being heated at 95°C, CD spectrum was partially recovered, indicating an incomplete reversibility of the unfolding/refolding process. The irreversibility was probably caused by the aggregation of the heat-unfolded protein. Furthermore, the thermal denaturation curves were used to compare the stabilities among platinated proteins and the melting temperatures (Tm) were summarized in the inset (Fig. 18). The results showed that the melting temperatures of BRCA1 were about 74°C and 83°C in the absence and presence of Zn^{2+}, respectively. This suggested that the BRCA1 RING domain was more thermostable by about 9°C upon Zn^{2+} binding. Thus, it supported the important role of Zn^{2+} in the determination and stabilization of the local secondary structure in the RING domain. It was notably that cisplatin at the concentration of 10 μM exhibited similar melting temperatures as those observed for Zn^{2+} binding to the BRCA1 RING domain. However, higher melting temperatures were observed at a 10-fold concentration of cisplatin. These data suggested that cisplatin binding to the BRCA1 RING domain conferred an enchanced thermostability by 13°C. Resistance to thermal denaturation of cisplatin-modifed BRCA1 RING domain might result from the favourably intermolecular crosslinks driven by the free energy.

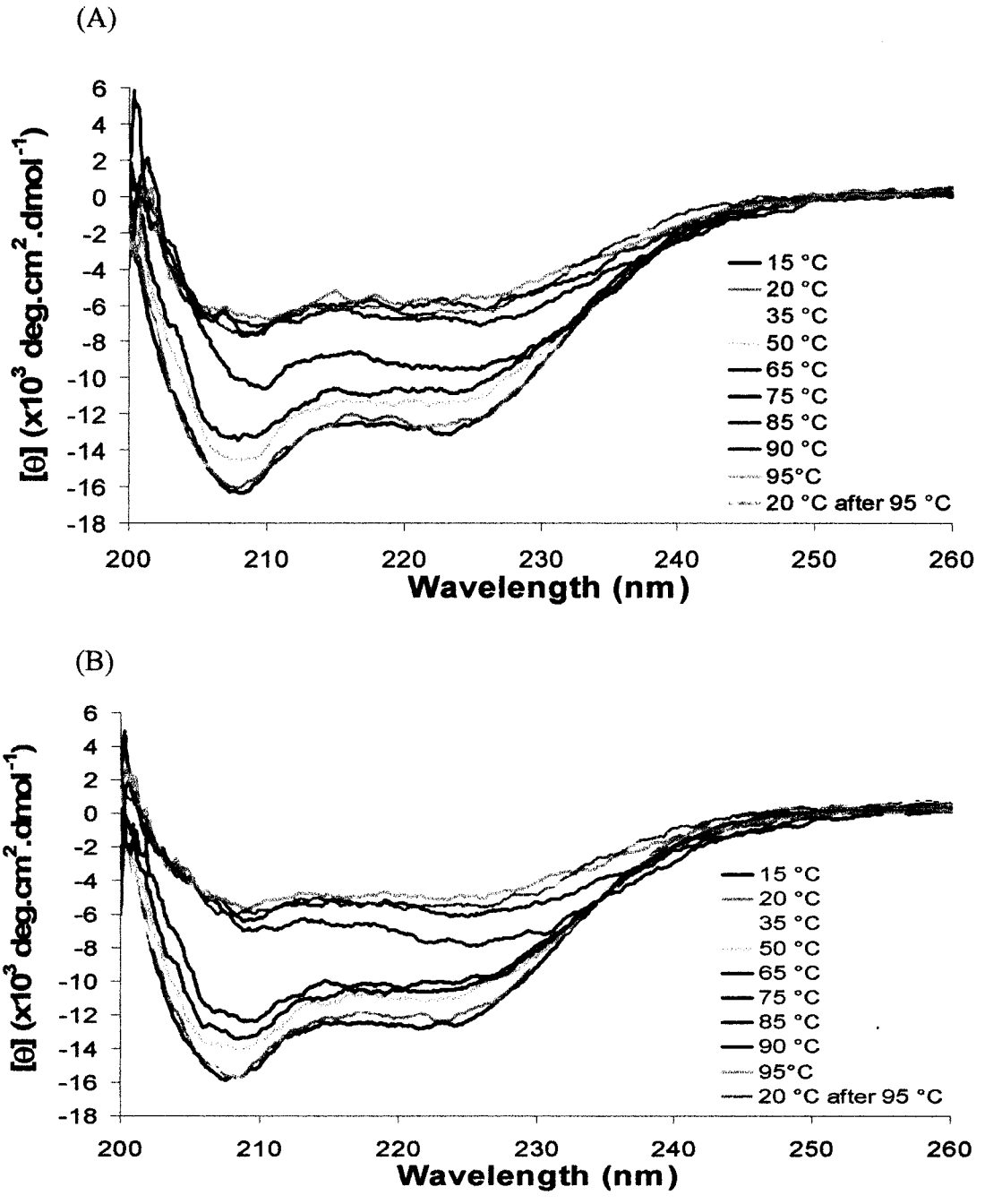

Figure 17. Thermal transition of cisplation-BRCA1 adducts. BRCA1 proteins (10 μM) without Zn^{2+} (A) and with pre-incubation of 3 mol-equiv. ratio of Zn^{2+} to protein (B) were mixed with an equivalent ratio of cisplatin. Samples were incubated in the dark at ambient temperature for 24 h and monitored by the far-UV-CD at defined temperatures. The measurements were performed from 15°C to 95°C with a heating rate of 1°C/min. After heating at 95°C, the measurement at 20°C was also performed. The CD spectra were plotted between mean residue ellipticity and wavelength.

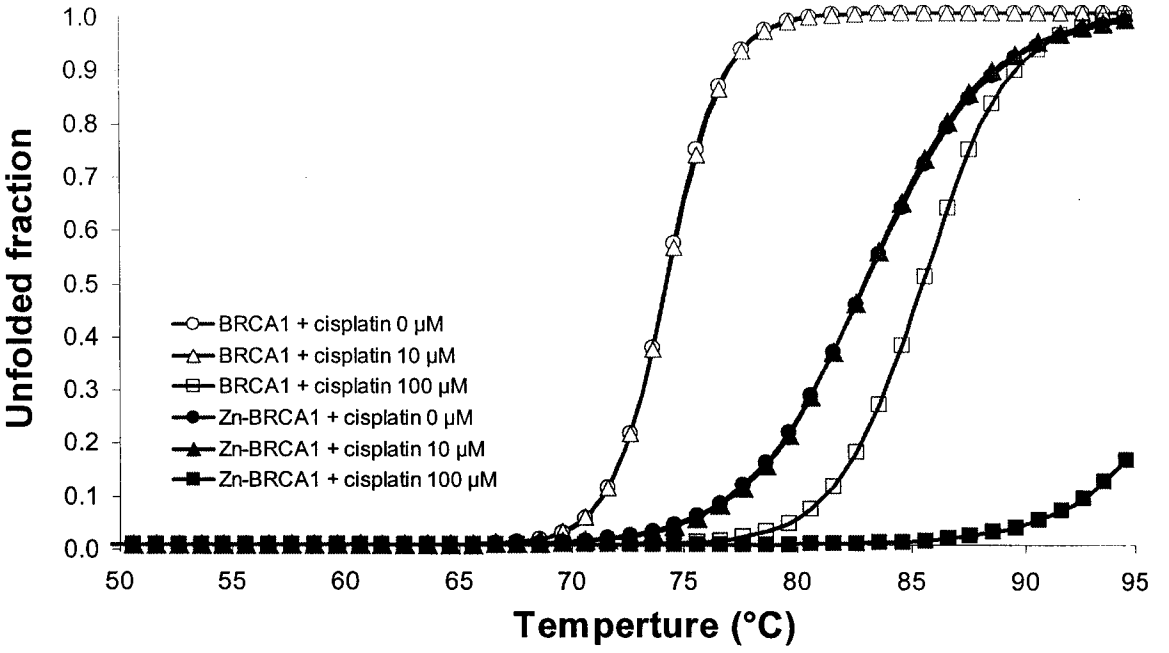

Figure 18. Thermal denaturation curves of cisplatin-BRCA1 adducts. BRCA1 protein (10 μM) without Zn^{2+} and with pre-incubation of 3 mol-equiv. ratio of Zn^{2+} to protein were mixed with various concentrations of cisplatin (0, 10, and 100 μM). Samples were incubated in the dark at ambient temperature for 24 h before CD measurement. The CD signals at 208 nm were measured, and the unfolded fraction as a function of temperature was plotted.

DISCUSSION

The interactions of some proteins with cisplatin have extensively been investigated and the cisplatin-protein adducts are divergent in the formations and functions. For instance, the platination of human serum albumin caused a partial unfolding of the protein structure at high drug concentration and induced intermolecular crosslinks [8,11]. A few types of intramolecular crosslinks were also occurred in ubiquitin adducts [13]. The loss activity in protein aggregation prevention of the C-terminal heat shock protein 90 was reported as the consequence of cisplatin binding but it did not show any conformational change [54].

Numerous studies of BRCA1 have revealed its involvement in DNA repair whose functional loss results in increased anticancer activities of some DNA damaging chemotherapeutics [35-38]. Targeting cancer cells specifically by utilizing the advantage of BRCA1 inactivation could provide an effectively clinical response with lesser adverse effects for treatment of BRCA1-associated cancers and their acquired resistance [35,55]. In the present study, the BRCA1 RING domain was targeted by the anticancer drug cisplatin and its structural consequences of protein conformation and thermal denaturation were observed. The RING protein revealed some structural elements in its apo-form and additional folded structure in the holo-form. Not only was the structure more folded or compacted upon metal binding, but the protein coordinating with Zn^{2+} appeared to be resistant to proteolysis. This was in correlation to other Zn^{2+} finger proteins such as transcription factor IIIA, exhibiting the metal-dependent folding recognized in the RING domain family to provide the proper conformation for interactions with other macromolecules [56].

Cisplatin-modified RING protein presented herein revealed favourably mono- and bifunctional BRCA1 adducts. Binding of cisplatin to the apo-form of BRCA1 underwent more folded structural rearrangement potentially at the vacant Zn^{2+}-binding sites. However, cisplatin did not perturb the global conformation of the holo-form of the BRCA1 RING protein. It implied that the drug interacted with other residues beyond the Zn^{2+}-binding sites. Tandem mass spectrometric analyses (MS/MS) indicated the formation of monofunctional adduct with $[Pt(NH_3)_2(OH)]^+$ on the BRCA1 peptide ^{111}ENNSPEHLK^{119}. The protonation of Lys119 at neutral pH and the preference of aquated cisplatin for His based on a dipeptide His-Ser model also

supported our result that His117 was the Pt-binding site [57]. Although the hydroxo form in the adduct complex is generally less reactive than the aqua form, its existence may be essential for interaction with other nucleophiles as it shows the significant reactivity towards thiol groups [58].

The Pt binding to BRCA1 gave the binding constant of $3.00x10^6$ M^{-1}, equivalent to that of Zn^{2+} binding ($2.79x10^6$ M^{-1}). The calculated free energy of cisplatin and Zn^{2+} bindings were about -8.68 and -8.64 kcal mol^{-1}, respectively, suggesting the thermodynamic contribution of metal-induced protein folding in the RING domain to drive protein folding, dimerization and thermostability of BRCA1. The comparison of these two binding constants was not straightforward as described in a previous study, demonstrating the affinity of Zn^{2+} and cisplatin to a short Zn^{2+} finger peptide of 31 mers in the different fashion [16]. Zn^{2+} binding to such a peptide employed the stepwise coordination by four cysteines with the binding constant of $3.91x10^4$ M^{-1}, whilst the Pt binding involved the coordination by two cysteines with the affinity of $8.80x10^4$ M^{-1}. However, the binding constant of the Pt-atom to a larger Zn^{2+} finger protein is suggested to be much higher due to other favourable binding sites beyond the Zn^{2+}-binding residues of protein. Moreover, a short synthetic peptide containing a minimal BRCA1 RING domain exhibited the Co^{2+} binding constants ranging from $1.26x10^5$ M^{-1} to $3.85x10^7$ M^{-1} [59]. Generally, the binding specificity of a Zn^{2+}-binding peptide for Co^{2+} was 2-4 orders of magnitude lower than that for Zn^{2+} [60-61]. Our observed binding constants are therefore consistent with these studies and showed a 34-fold higher Pt affinity than that observed for the short Zn^{2+} finger peptide of 31 mers ($3.00x10^6$ M^{-1} vs. $8.80x10^4$ M^{-1}), implying the overall influence of the adjacent residues of the RING protein on the metal affinity [16]. Additionally, the Zn^{2+}-bound BRCA1 RING domain was more thermostable by 9°C than the Zn^{2+}-free protein. The increased stability was apparently provided by the coordinating Zn^{2+}, which mostly contributed to the proper folding of BRCA1. Although the melting temperature of the BRCA1 RING domain was high and far from the physiological condition (about 74-83°C), it was consistent with the previous study, showing that the Zn^{2+} finger domain formed a thermostable structure [55,62]. Furthermore, the increased thermostability of cisplatin-BRCA1 adducts by 13°C probably resulted from the thermodynamically stabilizing contribution of intermolecular cross-links [63].

Cisplatin can interact nonspecifically with cellular proteins. Nucleophilic thiol proteins such as glutathione and metallothioneins are capable of binding to cisplatin before reaching the cellular targets. The intracellular concentration of glutathione is as high as 10 mM and it correlates to cisplatin resistance in which 1 mol of Pt binds to 2 mol of glutathione with the rate constant of 8.45×10^{-2} M^{-1} s^{-1} [64-65]. Moreover, the increased levels of metallothioneins have been found in some cisplatin-resistant cells [64]. The stoichiometry of cisplatin-metallothionein (7:1) complex is established with a significantly high association constant of 2.3×10^{23} M^{-1} [67]. The high abundance and affinity to Pt of both two proteins in cells can compete with the BRCA1 RING protein for cisplatin binding. To avoid cisplatin inactivation, some specific enzyme inhibitors for biosynthesis of glutathione and metallothioneins have been used [68]. Alternatively, a new generation of Pt-based drug such as picoplatin, currently in phase III trial, is also promising because of its steric hindrance around the Pt-center, reducing drug inactivation by these thiol-containing molecules [69-70].

However, the functional consequences of cisplatin-modified BRCA1 RING domain need to be further characterized as it has been shown to govern the ubiquitin ligase activity which closely associates with the DNA repair pathways [50]. The complete information would be beneficial for future therapeutic strategy of utilizing the BRCA1 N-terminal region as a potentially molecular target for Pt-based agents in the treatment of BRCA1-associated cancer and its aggressively basal-like and triple negative subtypes with higher survival rate [35-36].

CONCLUSION

Several investigations have gained much attention on taking advantage of the inherent weakness of the BRCA1 dysfunction in cancer therapy. Targeting the BRCA1 N-terminal domain through the disruption of Zn^{2+} coordination sites by the platinum-based drugs might be effective for the eradication of cancers and recurrent platinum-resistant cancers with lesser adverse effects than the empirical and conventional treatment. The cisplatin-modified BRCA1 N-terminal domain was capable of forming the formations of the favourably intramolecular and intermolecular protein adducts by which cisplatin binding to the apo form of BRCA1 induced more folded structural rearrangement potentially at the vacant Zn^{2+}-binding sites. Moreover, cisplatin did not perturb the global conformation of the holo form of the BRCA1 N-terminal domain, implying that cisplatin interacted with the other residues beyond the Zn^{2+}-binding sites. Cisplatin-modified BRCA1 also exhibited an enhanced thermostability, resulting from the favourably intermolecular cross-links driven by the free energy. The preferential platinum-binding site for the formation of the mono-molecular adduct between $[Pt(NH_3)_2(OH)]^+$ and the BRCA1 N-terminal domain was likely the His117. Taken together, the present data would provide a foundation for the utilization of the BRCA1 dysfunction, through the BRCA1 N-terminal domain, as a potentially molecular target for platinum-based drugs for significantly improving the efficacy in cancer therapy.

REFERENCES

[1] F. Muggia, *Gynecol. Oncol.* **2009**, *112*, 275.

[2] D. Wang, S. Lippard, *Nat. Rev. Drug Discov.* **2005**, *4*, 307.

[3] G.E. Damsma, A. Alt, F. Brueckner, T. Carell, P. Cramer, *Nat. Struct. Mol. Biol.* **2007**, *14*, 1127.

[4] A. Ratanaphan, S. Wasiksiri, B. Canyuk, P. Prasertsan, *Cancer Biol. Ther.* **2009**, *8*, 890.

[5] A. Ghezzi, M. Aceto, C. Cassino, E. Gabano, D. Osella, *J. Inorg. Biochem.* **2004**, *98*, 73.

[6] L. Cubo, D.S. Thomas, J. Zhang, A.G. Quiroga, C. Navarro-Ranninger, S.J. Berners-Price, *Inorg. Chim. Acta* **2009**, *362*, 1022

[7] P. Jordan, M. Carmo-Fonseca, *Cell. Mol. Life Sci.* **2000**, *57*, 1229.

[8] J.F. Neault, H.A. Tajmir-Riahi, *Biochim. Biophys. Acta* **1998**, *1384*, 153.

[9] L. Trynda-Lemiesz, H. Kozlowski, B.K. Keppler, *J. Inorg. Biochem.* **1999**, *77*, 141.

[10] I. Khalaila, C.S. Allardyce, C.S. Verma, P.J. Dyson, *Chem. Bio. Chem.* **2005**, *6*, 1788.

[11] A.I. Ivanov, J. Christodoulou, J.A. Parkinson, K.J. Barnham, A. Tucker, J. Woodrow, P.J. Sadler, *J. Biol. Chem.* **1998**, *273*, 14721.

[12] C.S. Allardyce, P.J. Dyson, J. Coffey, N. Johnson, *Rapid Commun. Mass Spectrom.* **2002**, *16*, 933.

[13] T. Peleg-Shulman, Y. Najajreh, D. Gibson, *J. Inorg. Biochem.* **2002**, *91*, 306.

[14] A. Casini, G. Mastrobuoni, C. Temperini, C. Gabbiani, S. Francese, G. Moneti, C.T. Supuran, A. Scozzafava, L. Messori, *Chem. Commun.* **2007**, *14*, 156.

[15] A. Casini, C. Gabbiani, G. Mastrobuoni, L. Messori, G. Moneti, G. Pieraccini, *Chem. Med. Chem.* **2006**, *1*, 413.

[16] R.N. Bose, W.W. Yang, F. Evanics, *Inorg. Chim. Acta* **2005**, *358*, 2844.

[17] R.A. Musah, *Curr. Top. Med. Chem.* **2004**, *4*, 1605.

[18] A.I. Anzellotti, Q. Liu, M.J. Bloemink, J.N. Scarsdale, N. Farrell, *Chem. Biol.* **2006**, *13*, 539.

[19] Q.A. de Paula, J.B. Mangrum, N.P. Farrell, *J. Inorg. Biochem.* **2009**, *103*, 1347.

[20] E.M. Rosen, S. Fan, R.G. Pestell, I.D. Goldberg, *J. Cell Physiol.* **2003**, *196*, 19.

[21] K. Gudmundsdottir, A. Ashworth, *Oncogene* **2006**, *25*, 5864.

[22] R.I. Yarden, M.Z. Papa, *Mol. Cancer Ther.* **2006**, *5*, 1396.

[23] P.S. Brzovic, P. Rajagopal, D.W. Hoyt, M.C. King, R.E. Klevit, *Nat. Struct. Biol.* **2001**, *8*, 833.

[24] C.-X. Deng, S.G. Brodie, *Bioassays* **2000**, *22*, 728.

[25] U.K. Westermark, M. Reyngold, A.B. Olshen, R. Baer, M. Jasin, M.E. Moynahan, *Mol. Cell. Biol.* **2003**, *23*, 7926.

[26] N. Turner, A. Tutt, A. Ashworth, *Curr. Opin. Pharmacol.* **2005**, *5*, 388.

[27] T. Helleday, E. Petermann, C.Lundin, B. Hodgson, R.A. Sharma, *Nat. Rev. Cancer* **2008**, *8*, 193.

[28] M.R. Kelley, M.L. Fishel, *Anticancer Agents Med. Chem.* **2008**, *8*, 417.

[29] M.E. Moynahan, J.W. Chiu, B.H. Koller, M. Jasin, *Mol. Cell* **1999**, *4*, 511.

[30] C.-X. Deng, R.-H. Wang, *Hum. Mol. Genet.* **2003**, *12*, R113.

[31] J.M. Stark, A.J. Pierce, J. Oh, A. Pastink, M. Jasin, *Mol. Cell. Biol.* **2004**, *24*, 9305.

[32] A. Bhattacharyya, U.S. Ear, B.H. Koller, R.R. Weichselbaum, D.K. Bishop, *J. Biol. Chem.* **2000**, *275*, 23899.

[33] P.O. Chappuis, J. Goffin, N. Wong, C. Perret, P. Ghadirian, P.N. Tonin, W.D. Foulkes, *J. Med. Genet.* **2002**, *39*, 608.

[34] P. Tassone, M.T.D. Martino, M. Ventura, A. Pietragalla, I. Cucinotto, T. Calimeri, P. Neri, M. Caraglia, P. Tagliaferri, *Cancer Biol. Ther.* **2009**, *8*, 648.

[35] T. Byrski, T. Huzarski, R. Dent, J. Gronwald, D. Zuziak, C. Cybulski, J. Kladny, B. Gorski, J. Lubinski, S.A. Narod, *Breast Cancer Res. Treat.* **2009**, *115*, 359.

[36] B. Sirohi, M. Arnedos, S. Popat, S. Ashley, A. Nerurkar, G. Walsh, S. Johnston, I.E. Smith, *Ann. Oncol.* **2008**, *19*, 1847.

[37] J.E. Quinn, R.D. Kennedy, P.B. Mullan, P.M. Gilmore, M. Carty, P.G. Johnston, D.P. Harkin, *Cancer Res.* **2003**, *63*, 6221.

[38] P. Tassone, P. Tagliaferri, A. Perricelli, S. Blotta, B. Quaresima, M.L. Martelli, A. Goel, V. Barbieri, F. Costanzo, C.R. Boland, S, Venuta, *Br. J. Cancer* **2003**, *88*, 1285.

[39] E.M. Swisher, W. Sakai, B.Y. Karlan, K. Wurz, N. Urban, T. Taniguchi, *Cancer Res.* **2008**, *68*, 2581.

[40] G. Damia, M. D'Incalci, *Eur. J. Cancer* **2007**, *43*, 1791.

[41] R. Litman, R. Gupta, R.M. Brosh Jr., S.B. Cantor, *Anticancer Agents Med. Chem.* **2008**, *8*, 426.

[42] S.D. Cosimo, J. Baselga, *Eur. J. Cancer* **2008**, *44*, 2781.

[43] S. Yi, J. Uhm, E. Cho, S. Lee, M. Park, H. Jun, Y. Park, J. Ahn, Y. Im, W. Kang, K. Park, *J. Clin. Oncol.* **2008**, *26(Suppl)*, 15s [Abstr 1008].

[44] J.E. Jaspers, S. Rottenberg, J. Jonkers, *Biochim. Biophys. Acta* **2009**, *1796*, 266.

[45] K. Rhiem, B. Wappenschmidt, K. Bosse, H. Köppler, A.N. Tutt, R.K. Schmutzler, *Clin. Oncol.* **2009**, *21*, 448.

[46] S.K. Pal, J. Mortimerb, *Maturitas* **2009**, *63*, 269.

[47] T. Byrski, M. Foszczynska-Kloda, T. Huzarski, R. Dent, J. Gronwald, C. Cybulski, T. Debniak, B. Gorski, J. Lubinski, S. Narod, *J. Clin. Oncol.* **2009**, *27(Suppl)*, 15s [Abstr 1099].

[48] P.S. Brzovic, J.E. Meza, M.-C. King, R.E. Klevit, *J. Biol. Chem.* **2001**, *276*, 41399.

[49] P.S. Brzovic, J.R. Keeffe, H. Nishikawa, K. Miyamoto, D. Fox III, M. Fukuda, T. Ohta, R. Klevit, *Proc. Natl. Acad. Sci. USA* **2003**, *100*, 5646.

[50] W. Wu, A. Koike, T. Takeshita, T. Ohta, *Cell Div.* **2008**, *3*, 1.

[51] S.W. Provencher, J. Glöckner, *Biochemistry* **1981**, *20*, 33.

[52] G. Engel, *Anal. Biochem.* **1974**, *61*, 184.

[53] S.J. Berners-Price, T.A. Frenkiel, U. Frey, J.D. Ranford, P.J. Sadler, *J. Chem. Soc., Chem. Commun.* **1992**, 789.

[54] R. Ishidaa, Y. Takaokaa, S. Yamamotoa, T. Miyazakia, M. Otakab, S. Watanabeb, A. Komatsudac, H. Wakuic, K. Sawadac, H. Kubotaa, H. Itoh, *FEBS Lett.* **2008**, *582*, 3879.

[55] I. Cass, R.L. Baldwin, T. Varkey, R. Moslehi, S.A. Narod, B.Y. Karlan, *Cancer* **2003**, *97*, 2187.

[56] A.D. Frankel, J.M. Berg, C.O. Pabo, *Proc. Natl. Acad. Sci. USA* **1987**, *84*, 4841.

[57] T. Zhao, F.L. King, *J. Inorg. Biochem.* **2010**, *104*, 186.

[58] M. El-Khateeb, T.G. Appleton, L.R. Gahan, B.G. Charles, S.J. Berners-Price, A.M. Bolton, *J. Inorg. Biochem.* **1999**, *77*, 13.

[59] P.C. Roehm, J.M. Berg, *Biochemistry* **1997**, *36*, 10240.

[60] B.A. Krizek, D.L. Merkle, J.M. Berg, *Inorg. Chem.* **1993**, *32*, 937.

[61] J.S. Magyar, H.A. Godwin, *Anal. Biochem.* **2003**, *320*, 39.

[62] J.M. Matthews, K. Kowalski, C.K. Liew, B.K. Sharpe, A.H. Fox, M. Crossley, J.P. Mackay, *Eur. J. Biochem.* **2000**, *267*, 1030.

[63] M.P. Byrne, W.E. Stites, *Protein Sci.* **1995**, *4*, 2545.

[64] R. Miao, G. Yang, Y. Miao, Y. Mei, J. Hong, C. Zhao, L. Zhu, *Rapid Commun. Mass Spectrom.* **2005**, *19*, 1031.

[65] D. Petrović, B. Stojimirović, B. Petrović, Z.M. Bugarčić, Ž.D. Bugarčić, *Bioorg. Med. Chem.* **2007**, *15*, 4203.

[66] M. Ebadi, P.L. Iversen, *Gen. Pharmacol.* **1994**, *25*, 1297.

[67] B.L. Zbang, W.Y. Sun, W. X. Tang, *J. Inorg. Biochem.* **1997**, *65*, 295.

[68] Y. Saga, H. Hashimoto, S. Yachiku, T. Iwata, M. Tokumitsu, *Int. J. Urol.* **2004**, *11*, 407.

[69] J.R. Eckardt, D.L. Bentsion, O.N. Lipatov, I.S. Polyakov, F.R. MacKintosh, D.A. Karlin, G.S. Baker, H.B. Breitz, *J. Clin. Oncol.* **2009**, *27*, 2046.

[70] J. Holford, F. Raynaud, B.A. Murrer, K. Grimaldi, J.A. Hartley, M. Abrams, L.R. Kelland, *Anticancer Drug Des.* **1998**, *13*, 1.